Vector Boson Scattering at the LHC

SM@LHC

Fermilab, July 10-13th, 2023

Saptaparna Bhattacharya

Spectrum of Standard Model measurements

Vector Boson Scattering processes produced with low cross section

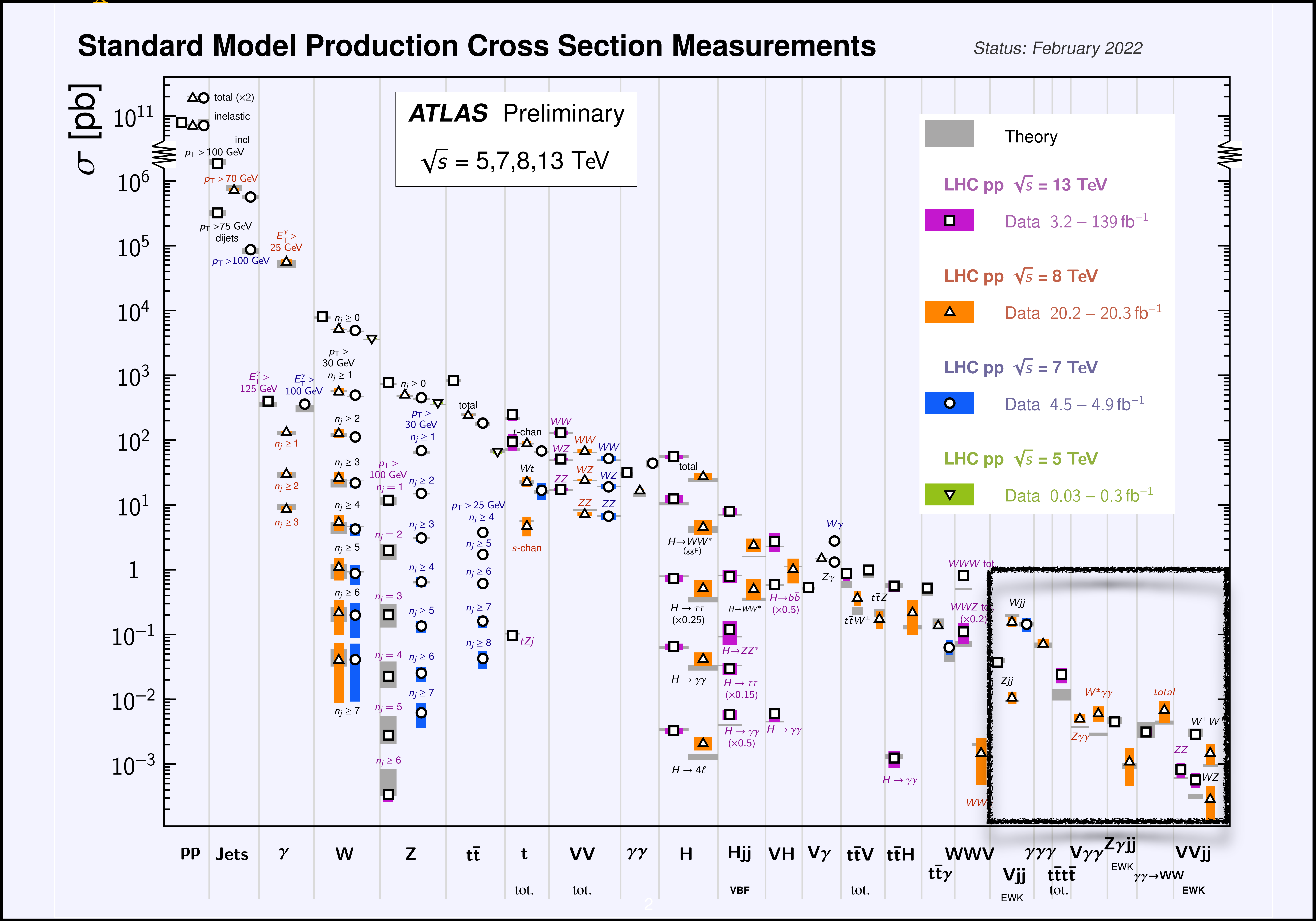

Multiboson cross sections span several orders of magnitude!

Vector Boson Scattering

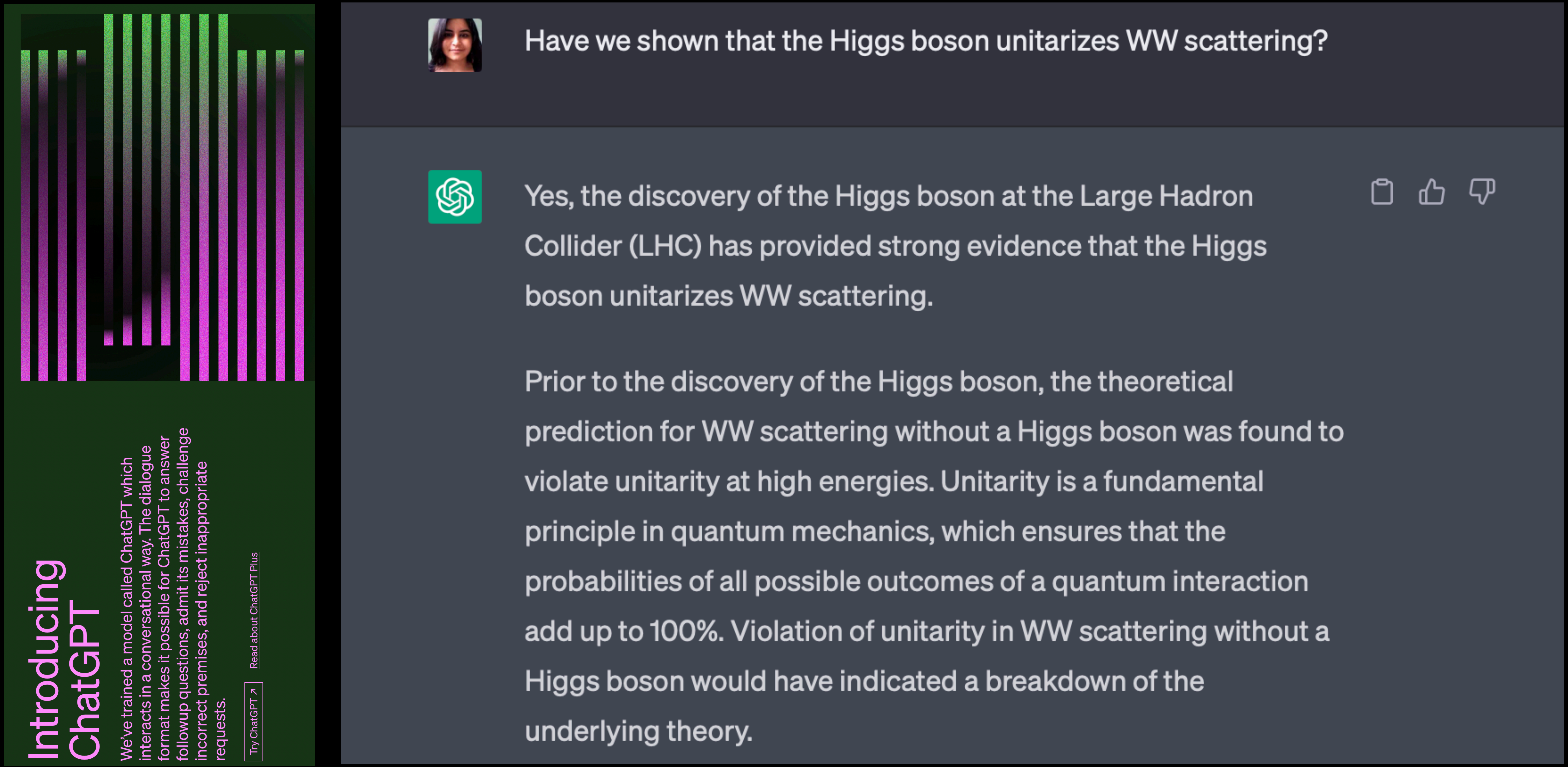

"However, it is important to note that the precise role of the Higgs boson in unitarizing WW scattering, in particular, is still an active area of research and there are ongoing studies to refine our understanding of this process."

Vector Boson Scattering

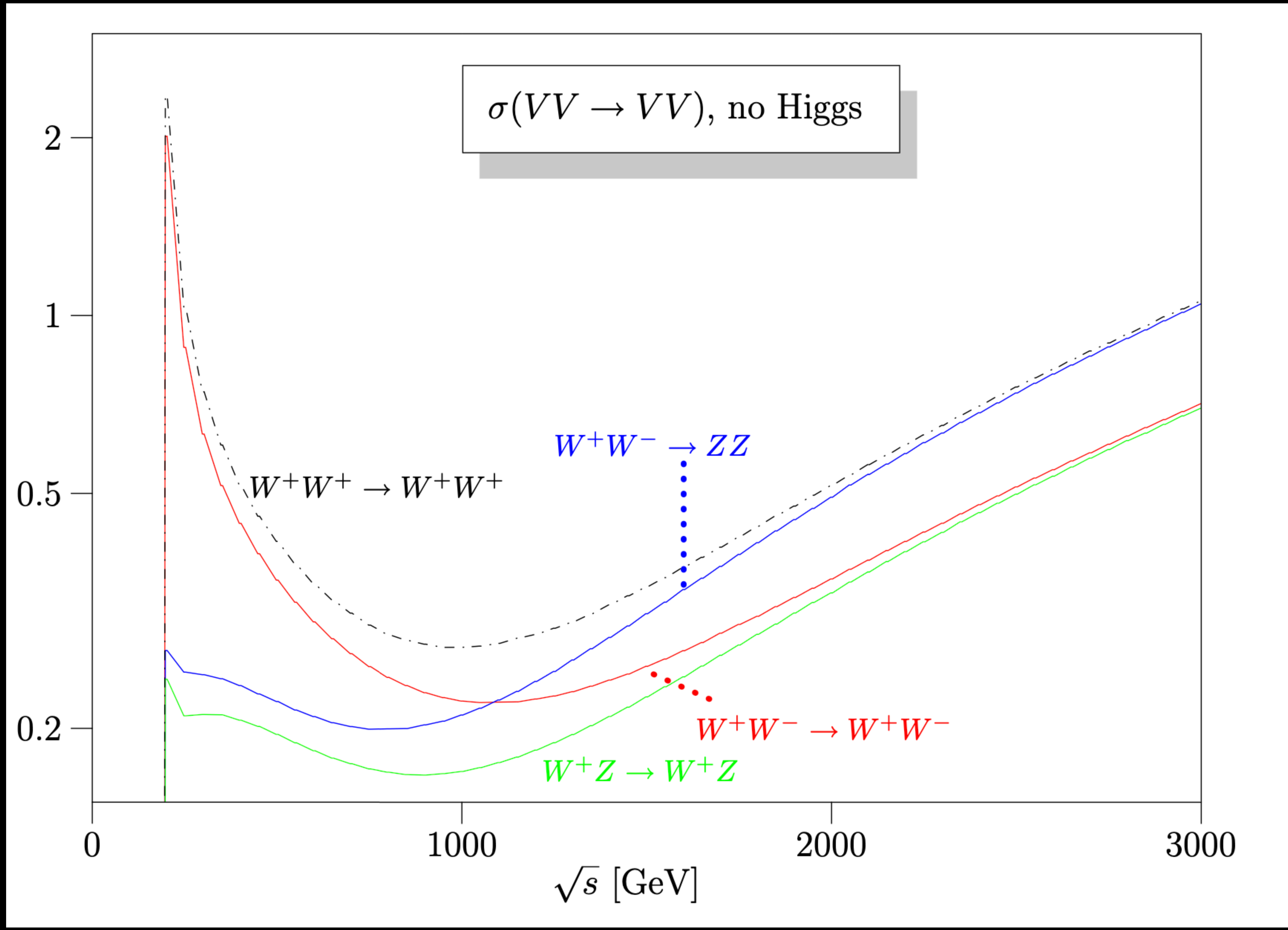

arXiv:0806.4145

"However, it is important to note that the precise role of the Higgs boson in unitarizing WW scattering, in particular, is still an active area of research and there are ongoing studies to refine our understanding of this process."

Vector Boson Scattering

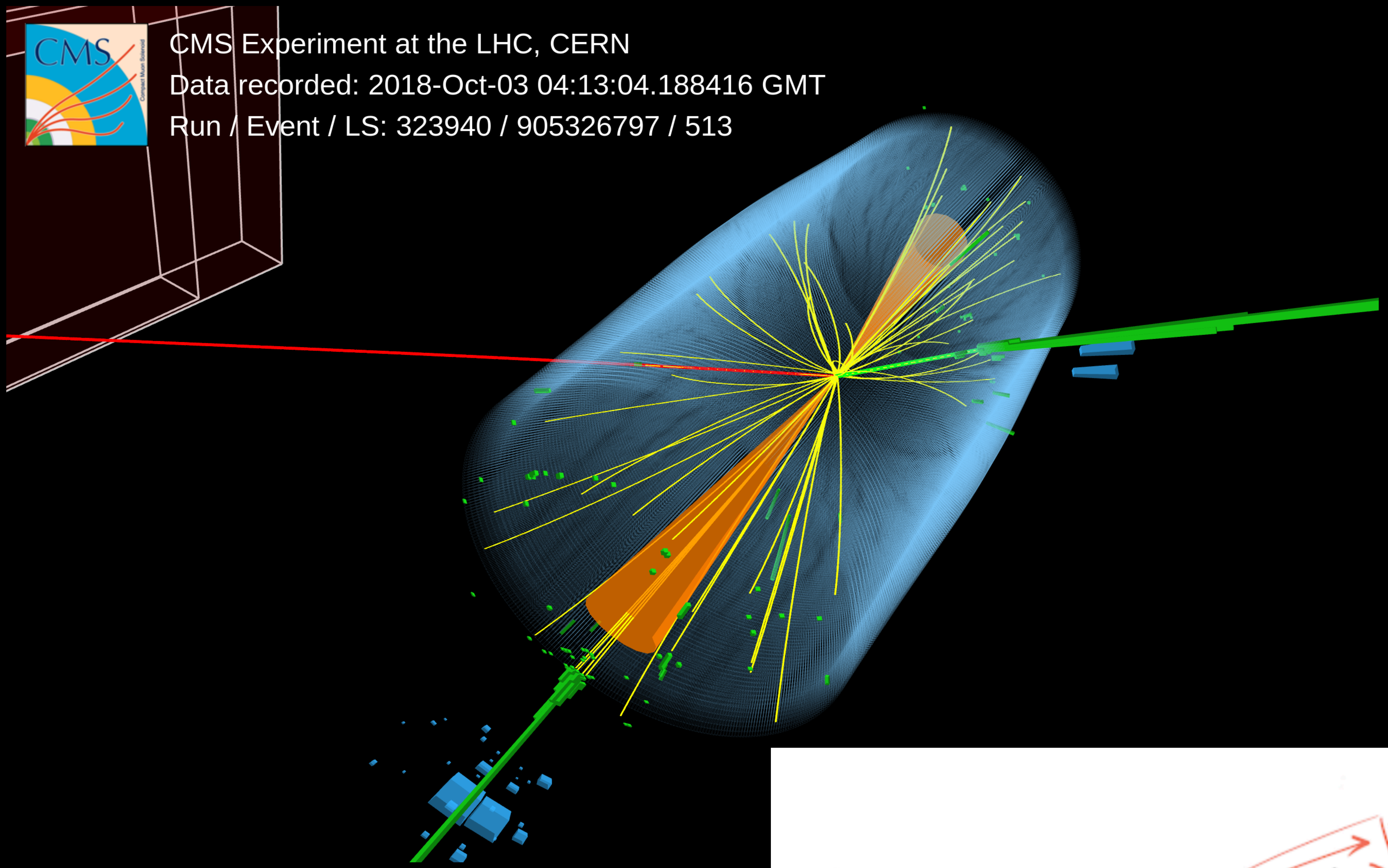

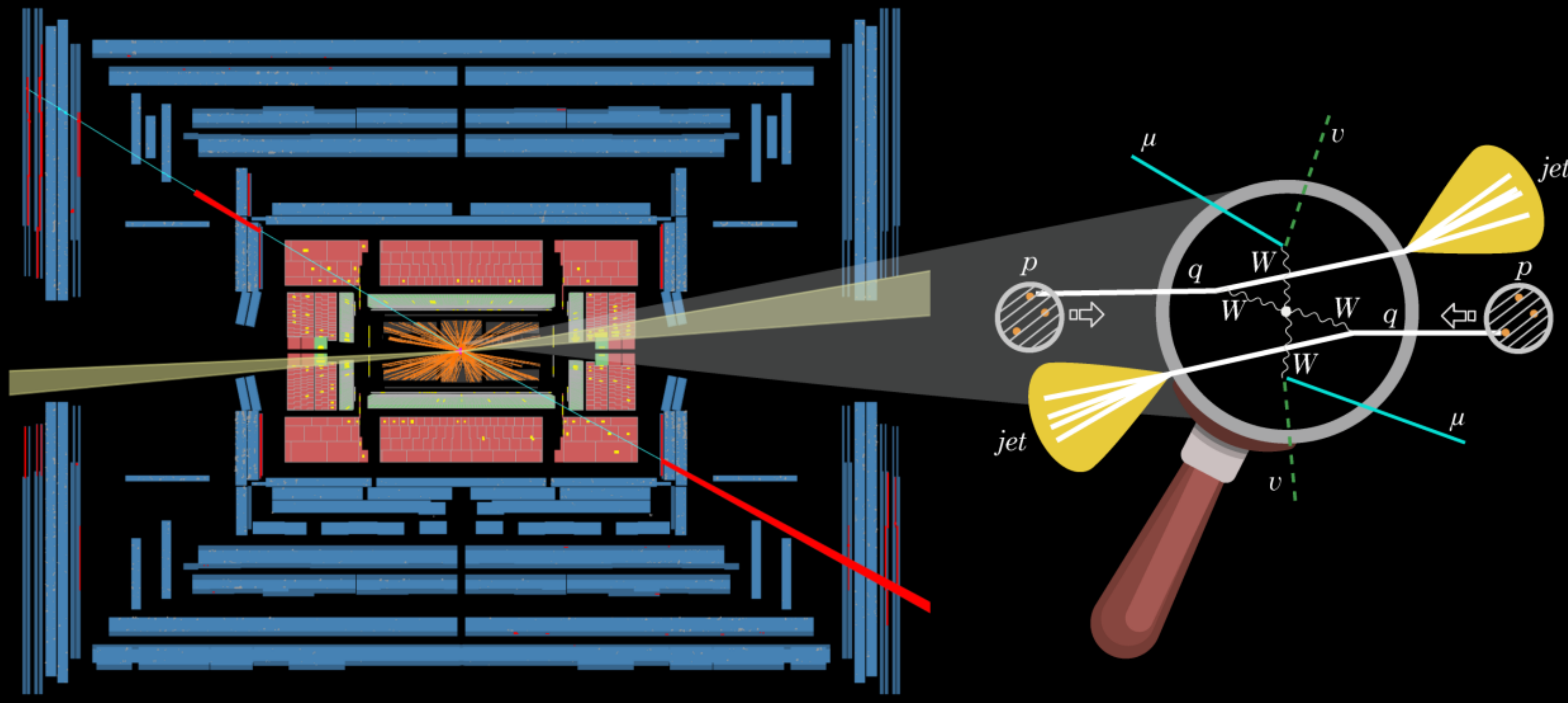

- Pure electro-weak interactions of order (α_{EW}^4)

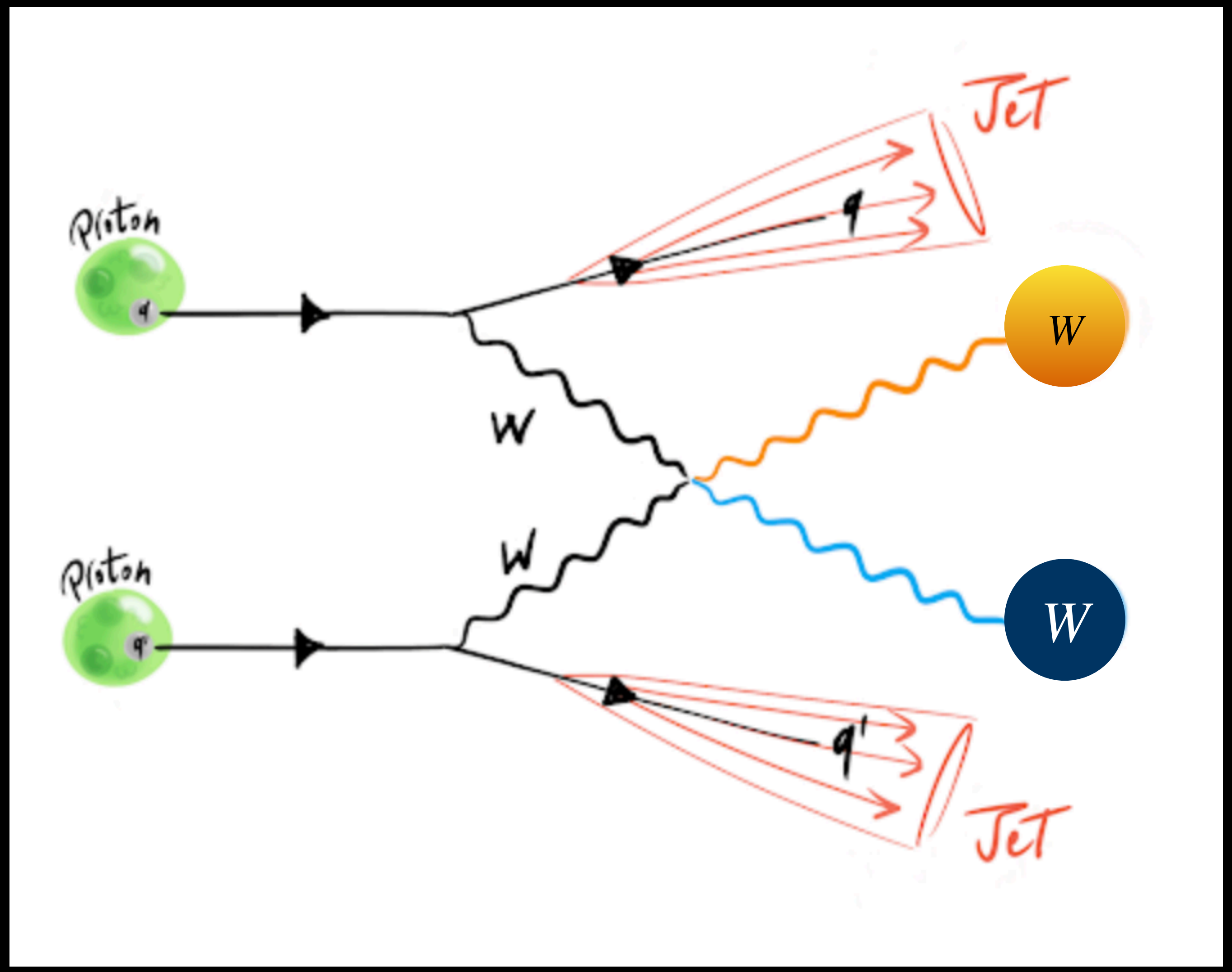

- Final state consists of two high transverse momenta (p_T) jets
- Rapidity gap between jets → no color flow
- High mass of the two jets (M_{jj})
- Decay product of the gauge bosons: central with respect to jets

Vector Boson Scattering — evolution of knowledge

ATLAS

$\sqrt{s}$	Process	Reference	Significance/Status
8 TeV	EW W±W±jj $(2\ell 2\nu jj)$	Phys. Rev. Lett. 113 (2014) 141803	3.6σ
	EW WVjj $(\ell\nu jjjj)$	Phys. Rev. D 95 (2017) 032001	Limits for aQGC*
	EW W±W±jj $(\ell\ell\nu\nu jj)$	Phys. Rev. D 96 (2017) 012007	Limits on aQGC*
	EW Zγjj $(\ell\ell jj/\nu\nu jj)$	JHEP 07 (2017) 107	2.0σ and limits on aQGC*
13 TeV	EW W±Zjj $(3\ell\nu jj)$	Phys. Lett. B 793 (2019) 469	5.3σ
	EW (WW,WZ,ZZ)jj $(\nu\nu jjjj, \ell\nu jjjj, \ell\ell jjjj)$	Phys. Rev. D 100 (2019) 032007	2.7σ
	EW W±W±jj $(\ell\ell jj)$	Phys. Rev. Lett. 123 (2019) 161801	6.5σ
	EW Zγjj $(\ell\ell\gamma jj)$	Phys. Lett. B 803 (2020) 135341	4.1σ
	W±W± $(\gamma\gamma \rightarrow W^+W^-)$	Phys. Lett. B 816 (2021) 136190	8.4σ
	EW ZZjj $(\ell\ell\ell\ell jj, \ell\ell 2\nu jj)$	Nature Phys. 19 (2023) 237	5.7σ
	EW Zγjj $(\nu\nu\gamma jj)$	JHEP 06 (2023) 082	6.3σ
	EW Zγjj $(\ell\ell\gamma jj)$	arXiv:2305.19142	> 5.0σ

*Anomalous quartic gauge coupling in Eboli basis with unitarity constraints applied

Electroweak production of a $Z\gamma$ pair in association with two jets

- First observation of electroweak $Z\gamma jj$ where Z decays to $\ell^+\ell^-, \ell = (e, \mu)$
- Probe of neutral quartic gauge coupling
- Fiducial and differential cross section measurements in several observables

Variable	Sensitive to
Transverse momenta of the leading lepton (p_T^l)	Generator modeling
Properties of the leading jets • Invariant mass (m_{jj}) • Absolute rapidity difference (|Δy|)	Kinematic differences of electroweak vs. QCD induced production of $Z\gamma jj$
Transverse momentum of the photon (E_T^γ) and the $Z\gamma$ systems ($p_T^{Z\gamma}$), absolute azimuthal difference between the $Z\gamma$ system and the two jets ($\|\Delta\phi(Z\gamma, jj)\|$)	Potential new physics

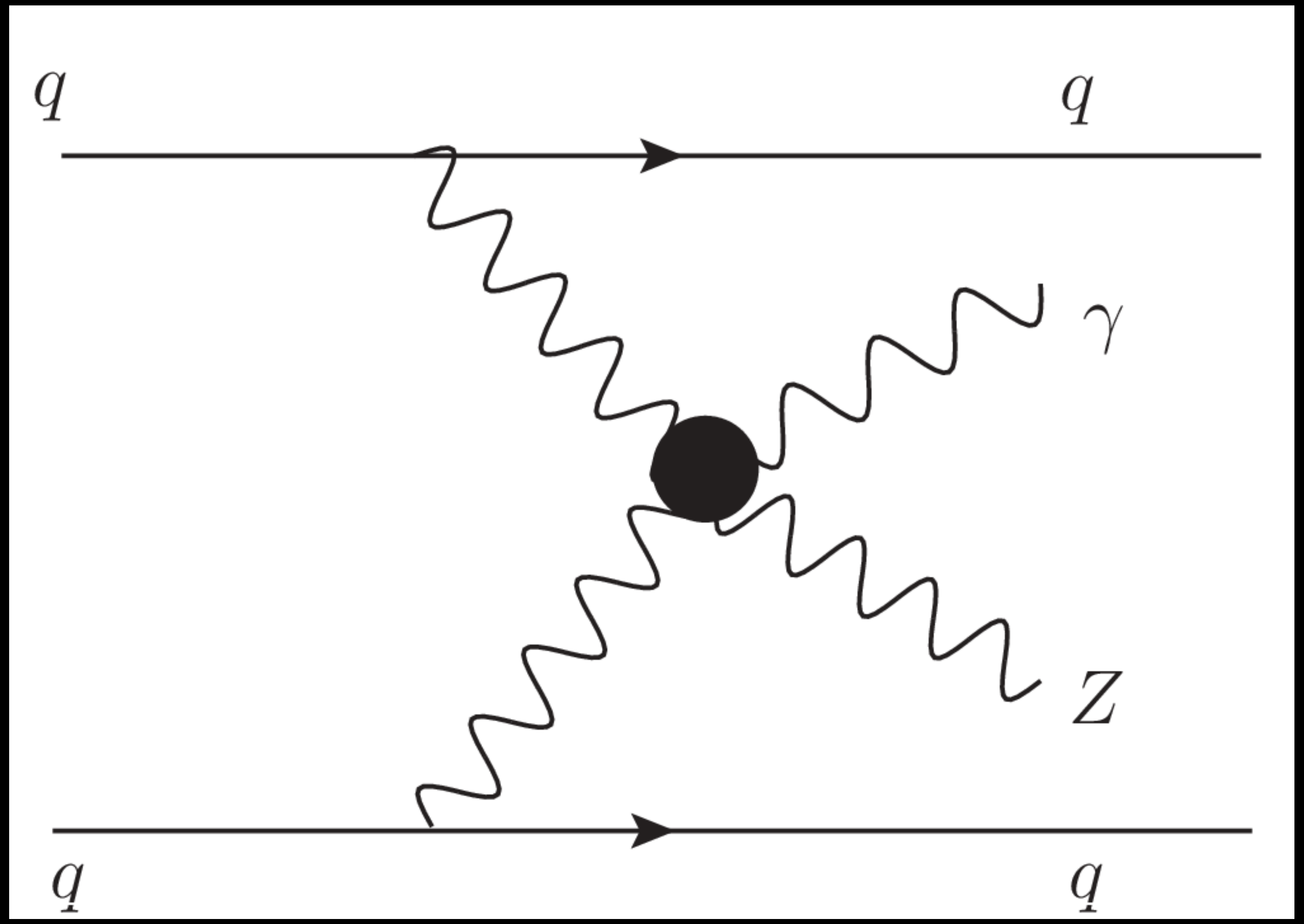

Lepton	$p_T^\ell > 20, 30(\text{leading})$ GeV, $\|\eta_\ell\| < 2.5$ $N_\ell \geq 2$
Photon	$E_T^\gamma > 25$ GeV, $\|\eta_\gamma\| < 2.37$ $E_T^{\text{cone20}} < 0.07 E_T^\gamma$ $\Delta R(\ell, \gamma) > 0.4$
Jet	$p_T^j > 50$ GeV, $\|y_j\| < 4.4$ $\|\Delta y\| > 1.0$ $m_{jj} > 150$ GeV or $m_{jj} > 500$ GeV Remove jets if $\Delta R(\gamma, j) < 0.4$ or if $\Delta R(\ell, j) < 0.3$
Event	$m_{\ell\ell} > 40$ GeV $m_{\ell\ell} + m_{\ell\ell\gamma} > 182$ GeV $\zeta(Z\gamma) < 0.4$ $N_{\text{jets}}^{\text{gap}} = 0$

Electroweak production of a $Z\gamma$ pair in association with two jets

- EW $Z\gamma jj$ differential cross-section as a function of the invariant mass of the two jets → important variable for extracting electroweak component and suppressing QCD-induced component of production
  - Cross section measured with 13% precision 3.6 ± 0.5 fb, differential cross sections measured with 20% average precision
- Extending signal region to include QCD-induced $Z\gamma jj$ mode to study $p_T^{Z\gamma}$ → to study contributions from higher order operators
  - Cross section: $16.8^{+2.0}_{-1.8}$ fb, compare with Madgraph_aMC@NLO 2.6.5 + SHERPA 2.2.11: $15.7^{+5.0}_{-2.6}$ fb

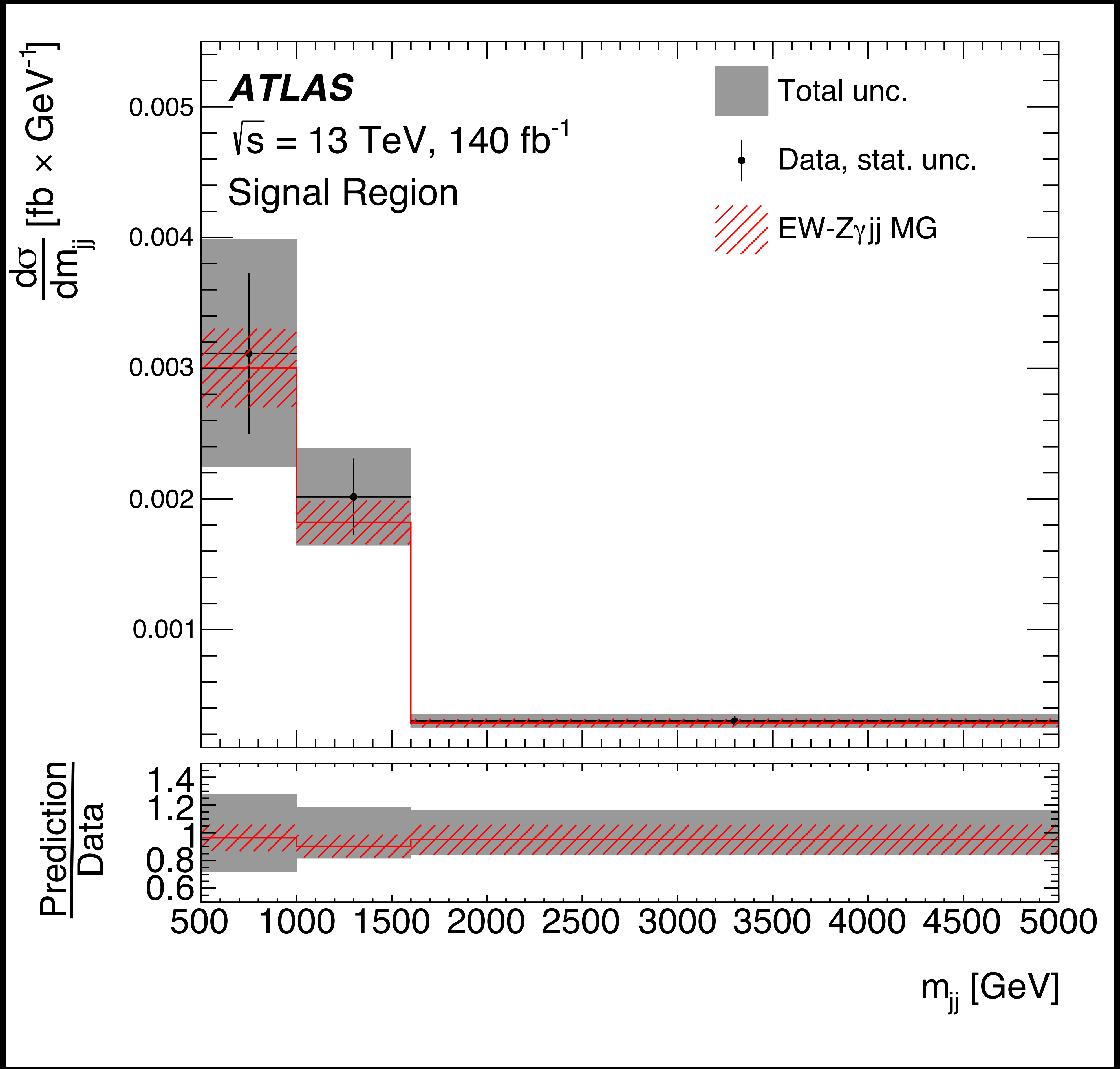

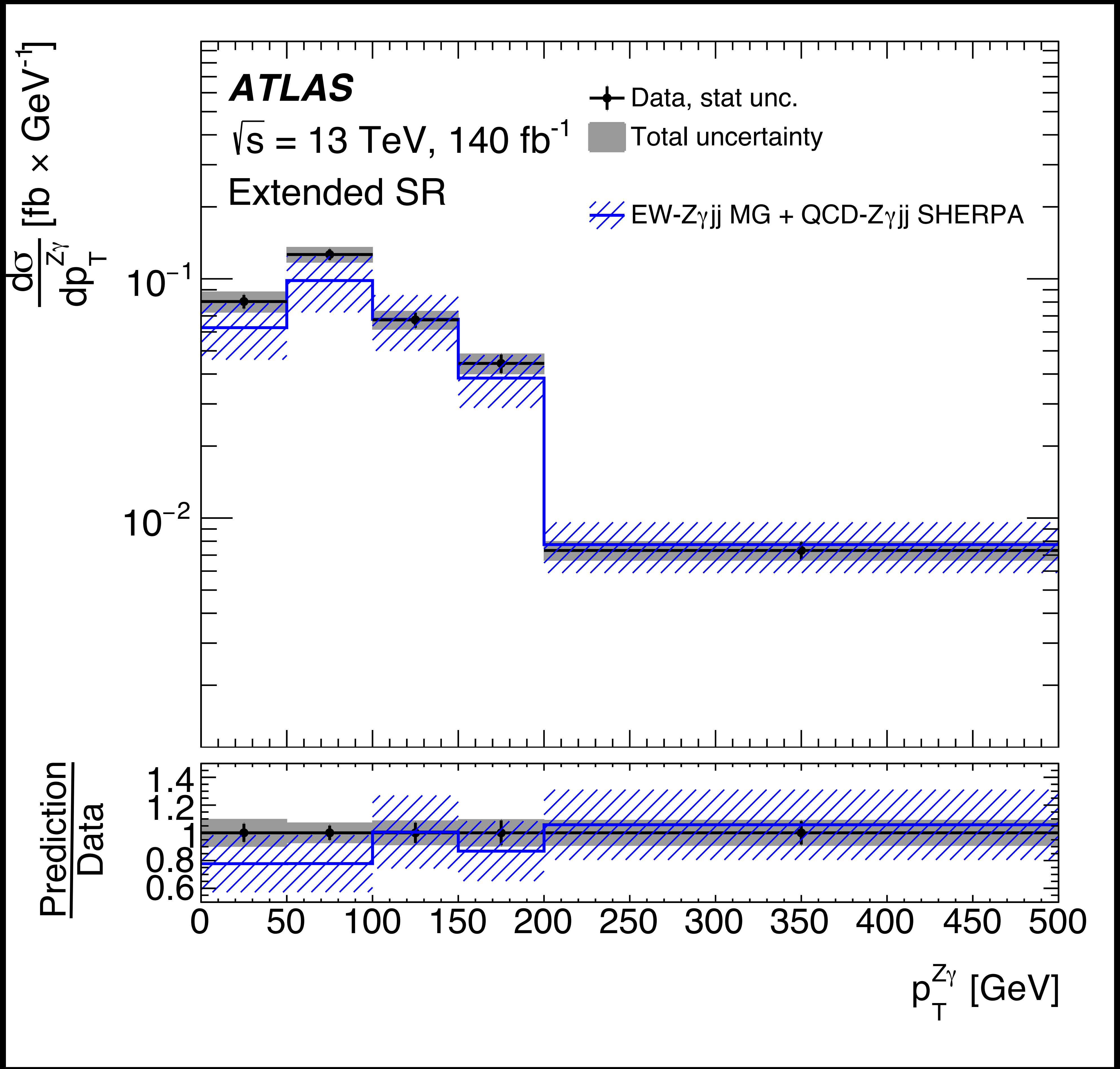

Measurements of Zγ+jets differential cross sections

- Evidence of electroweak Zγjj where Z decays to $\nu\bar{\nu}$
  - Observed (expected) significance of 3.2σ (3.7σ)
  - Combination with previous result: 6.3σ (6.6σ)
- Constraints set on anomalous quartic couplings

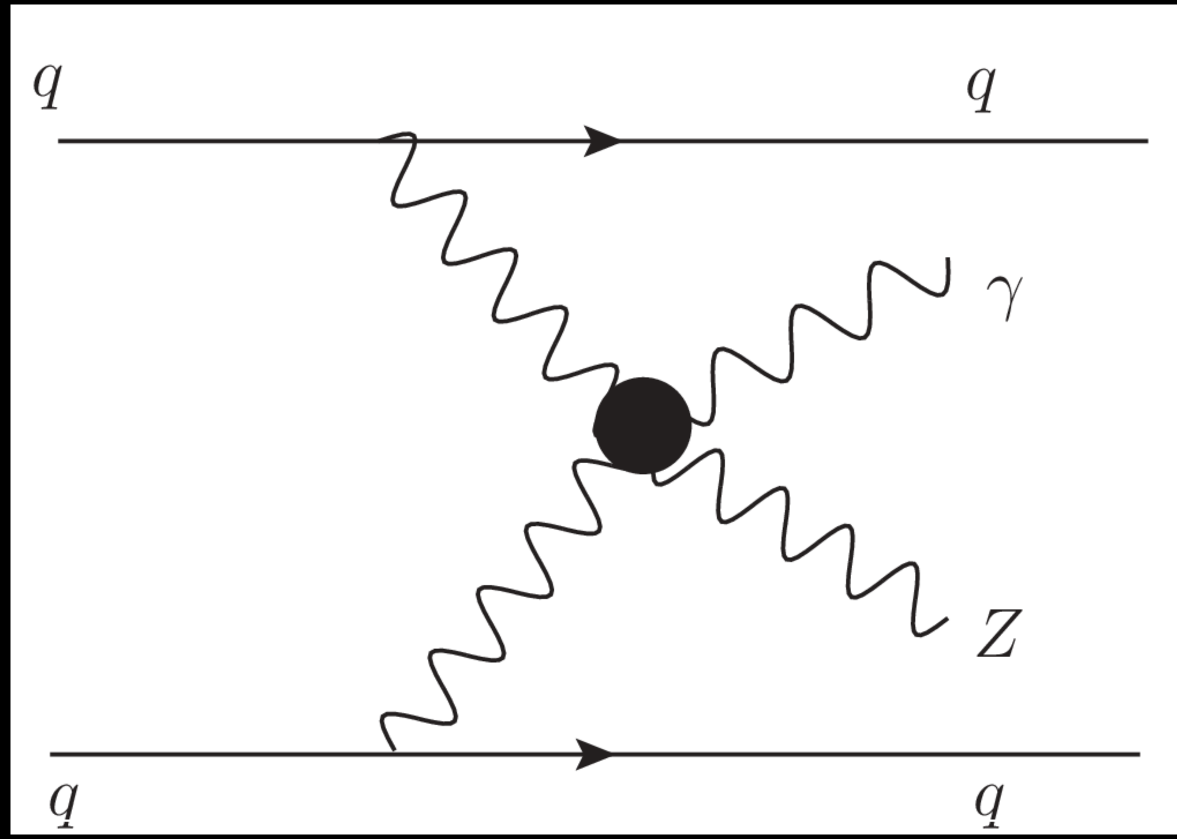

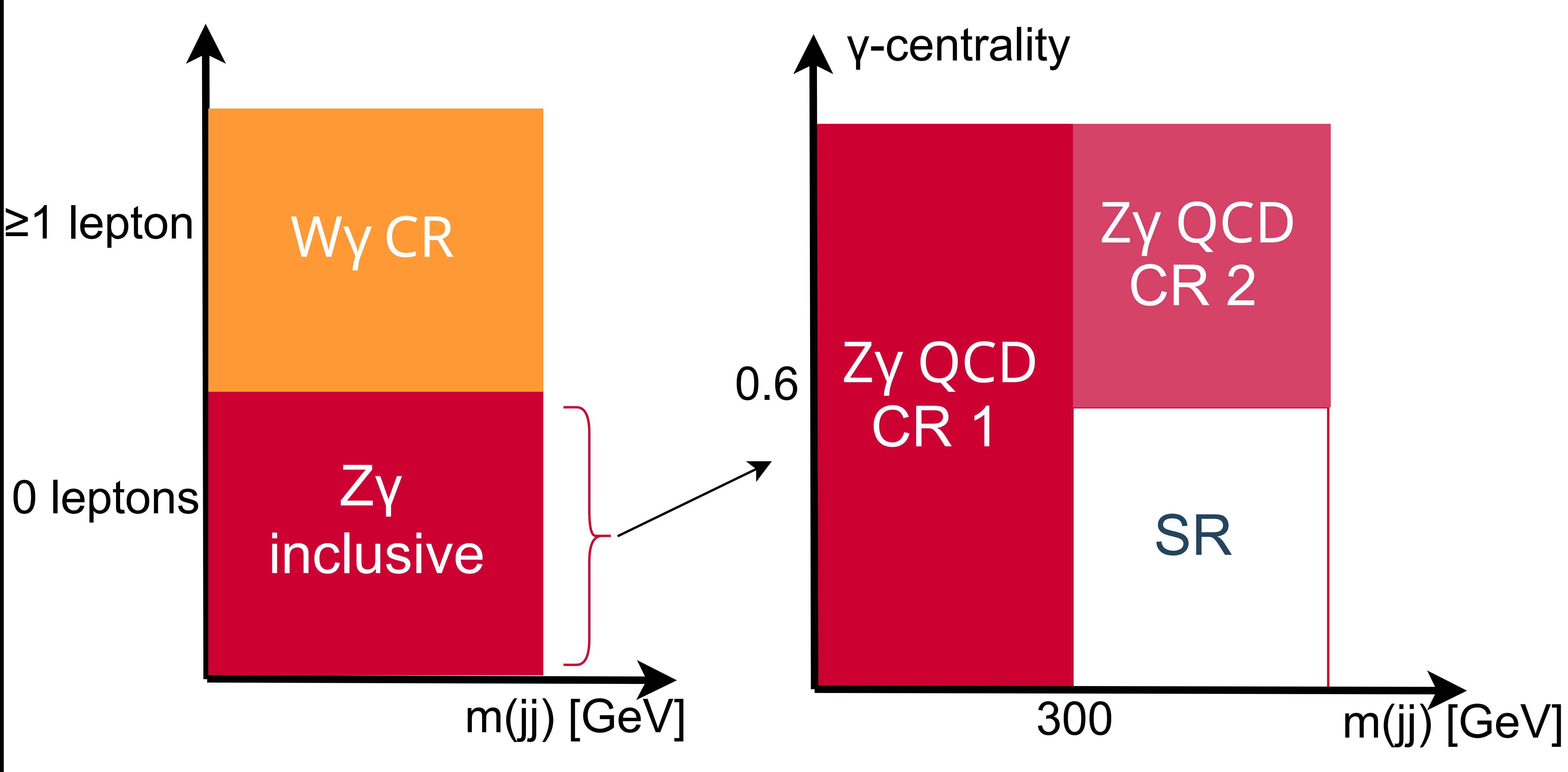

Selections	Cut value
E_T^{miss}	> 120 GeV
E_T^{γ}	> 150 GeV
Number of isolated photons	$N_\gamma = 1$
Photon isolation	$E_T^{cone40} < 0.022 p_T + 2.45$ GeV, $p_T^{cone20}/p_T < 0.05$
Number of jets	$N_{jets} \geq 2$ with $p_T > 50$ GeV
Overlap removal	$\Delta R(\gamma, \text{jet}) > 0.3$
Lepton veto	$N_e = 0$, $N_\mu = 0$
$\lvert\Delta\phi(\gamma, \vec{p}_T^{miss})\rvert$	> 0.4
$\lvert\Delta\phi(j_1, \vec{p}_T^{miss})\rvert$	> 0.3
$\lvert\Delta\phi(j_2, \vec{p}_T^{miss})\rvert$	> 0.3
m_{jj}	> 300 GeV
γ-centrality	< 0.6

Measurements of $Z\gamma$+jets differential cross sections

- Boosted Decision Tree trained with (indicative):
  - m_{jj}, $\Delta y(j_1,j_2)$, E_T^{miss}, p_T-balance, η_{j_2}, $p_T(j_1)$,$\eta(\gamma)$,N_{jets},$\sin(|\Delta\phi(j_1,j_2)/2|)$ and $\Delta y(j_1,\gamma)$

$$p_T\text{-balance} = \frac{|\vec{p}_T^{\,\text{miss}} + \vec{p}_T^{\,\gamma} + \vec{p}_T^{\,j_1} + \vec{p}_T^{\,j_2}|}{E_T^{\text{miss}} + E_T^{\gamma} + \vec{p}_T^{\,j_1} + \vec{p}_T^{\,j_2}}$$

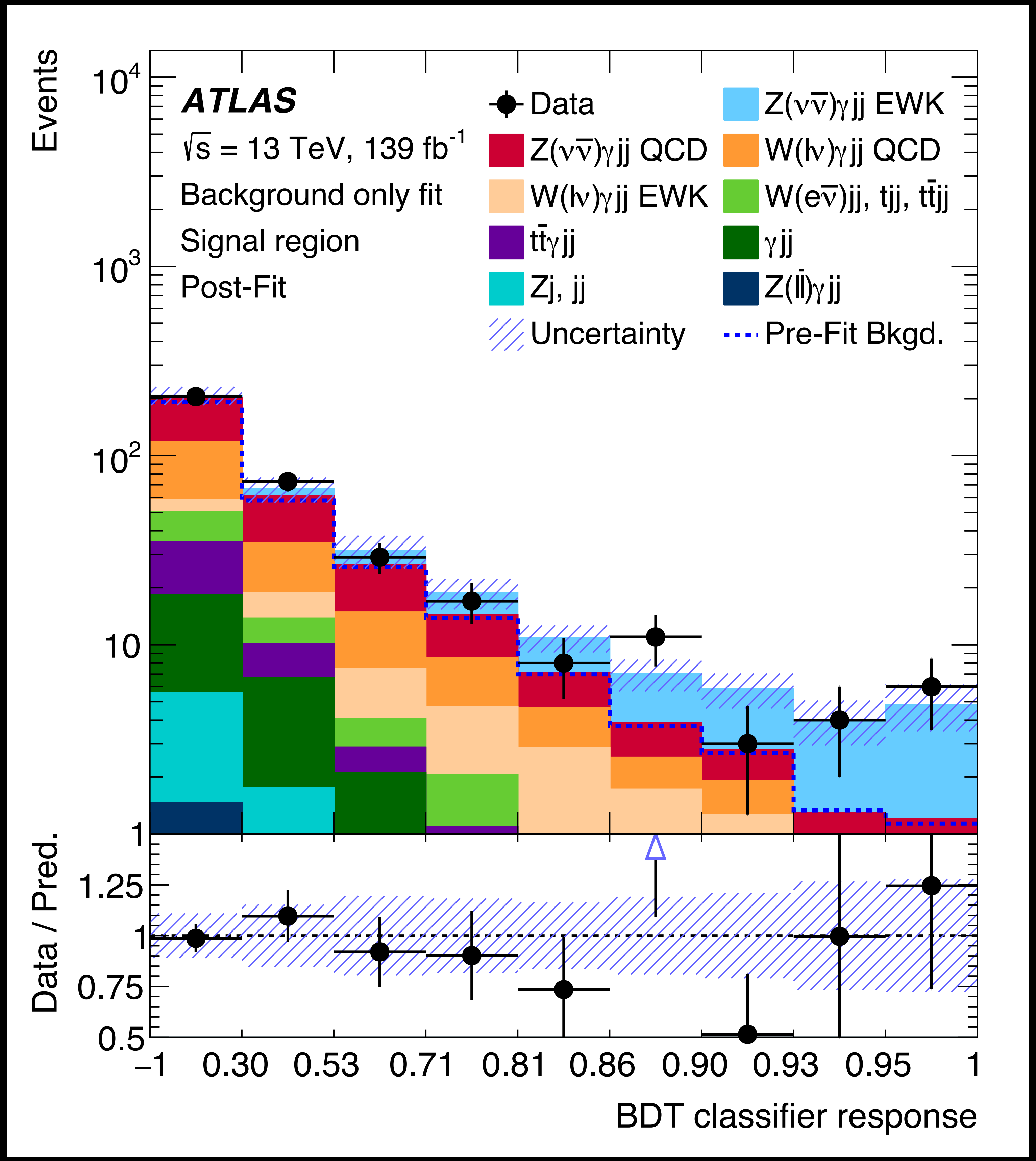

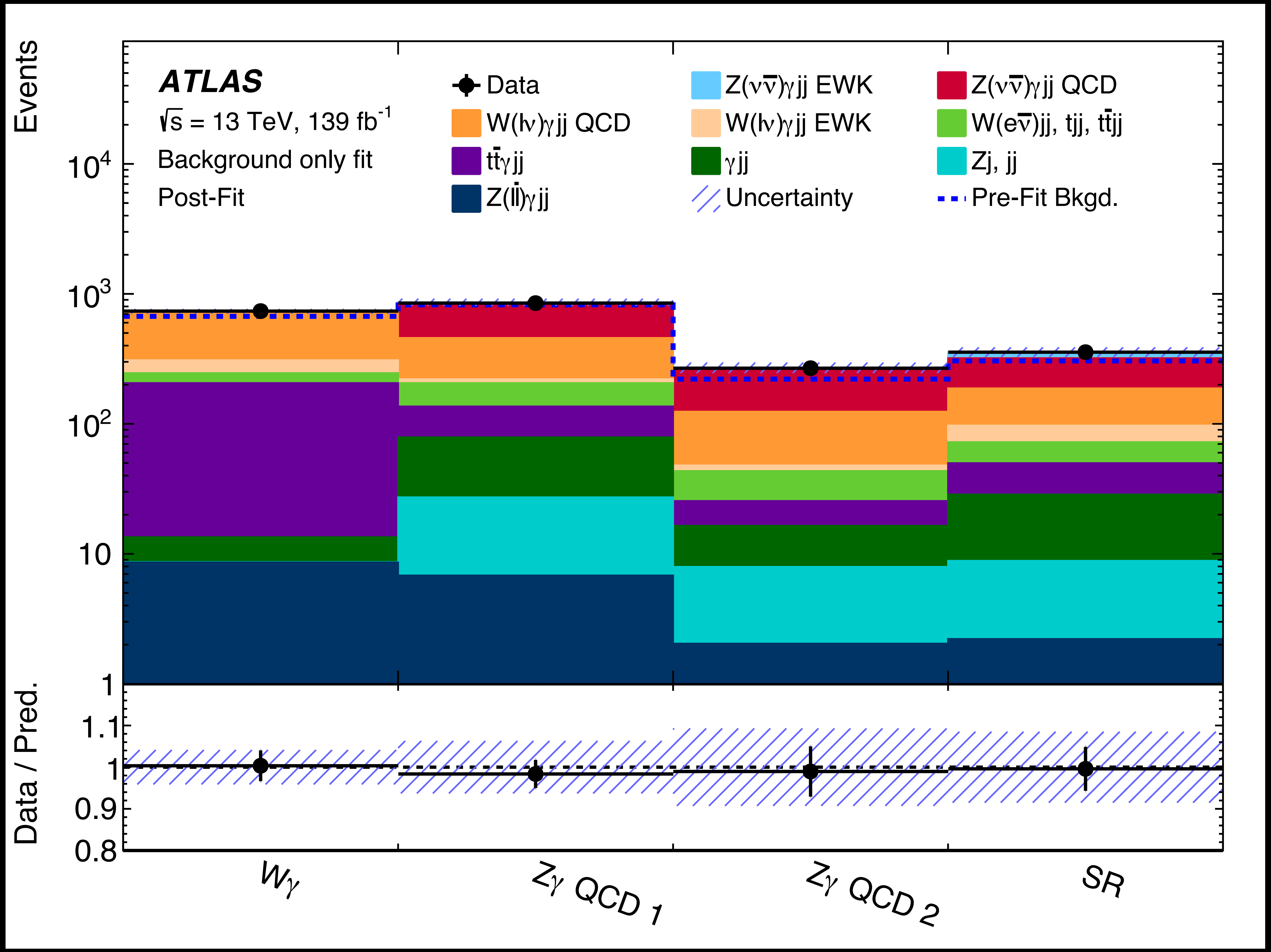

Measurements of $Z\gamma$+jets differential cross sections

- Large theoretical systematic uncertainty associated with signal modeling resulting from
  - renormalisation and factorisation scales
  - underlying event and parton showering or generator choice
- Pileup and E_T^{miss} modeling large contributor of experimental uncertainty

	$W\gamma$ CR	$Z\gamma$ QCD CR 1	$Z\gamma$ QCD CR 2	Signal region
$Z(\nu\bar{\nu})\gamma jj$ EWK	0.108 ± 0.028	11.0 ± 4.3	4.0 ± 2.2	37 ± 14
$Z(\nu\bar{\nu})\gamma jj$ QCD	1.04 ± 0.46	394 ± 84	143 ± 32	133 ± 39
$W(\ell\nu)\gamma jj$ QCD	425 ± 63	237 ± 71	76 ± 24	91 ± 30
$W(\ell\nu)\gamma jj$ EWK	63 ± 12	14.3 ± 2.7	4.5 ± 1.2	24.6 ± 4.9
$W(e\nu)jj, tjj, t\bar{t}jj$	39.8 ± 2.5	70.1 ± 4.1	17.9 ± 1.3	22.5 ± 1.5
$t\bar{t}\gamma jj$	193 ± 57	57 ± 20	9.1 ± 3.4	21.3 ± 7.6
γjj	4.8 ± 7.4	52 ± 36	8 ± 11	20 ± 17
Zj, jj	0.06 ± 0.66	20 ± 14	5.9 ± 6.9	6.6 ± 7.8
$Z(\ell\bar{\ell})\gamma jj$	8.6 ± 2.5	6.8 ± 2.0	2.04 ± 0.95	2.2 ± 1.3
Total	735 ± 30	863 ± 54	271 ± 25	357 ± 30
Data	737	849	268	356

Observation of electroweak production of two jets and a Z-boson pair

- Unique feature of fully reconstructed final state
- Probe of properties of the VBS process that are sensitive to electro-weak symmetry breaking
- VBS ZZ sensitive to possible anomalous interactions between two Z-bosons
- Precision tests of the VBS ZZ production allows an almost model independent measurement of the Higgs width

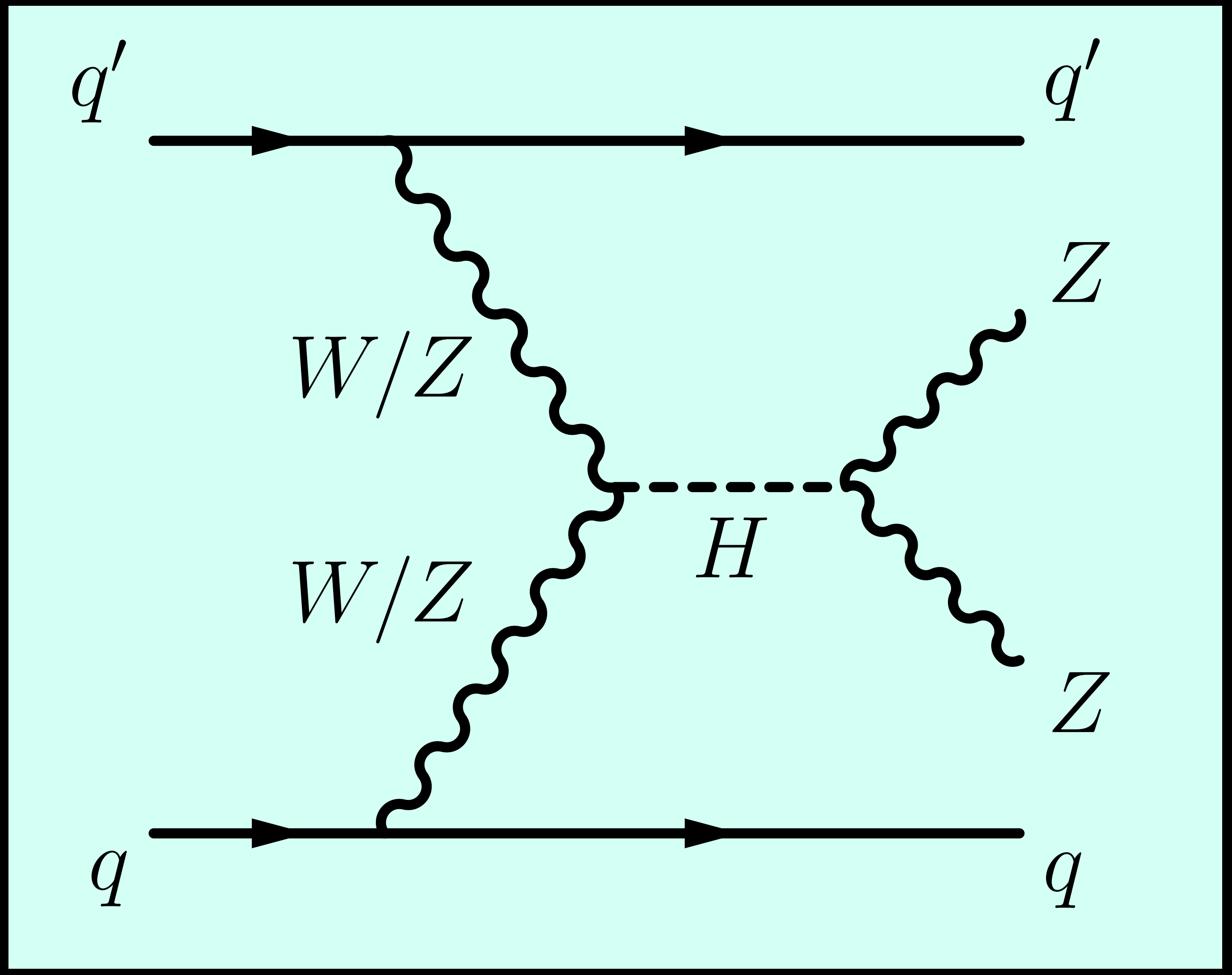

Process	$\ell\ell\ell\ell jj$	$\ell\ell\nu\nu jj$
EW $ZZjj$	31.4 ± 3.5	15.0 ± 0.8
QCD $ZZjj$	77 ± 25	17.2 ± 3.5
QCD $ggZZjj$	13.1 ± 4.4	3.5 ± 1.1
Non-resonant-$\ell\ell$	–	21.4 ± 4.8
WZ	–	24.6 ± 1.1
Others	3.2 ± 2.1	1.2 ± 0.9
Total	124 ± 26	82.9 ± 6.4
Data	127	82

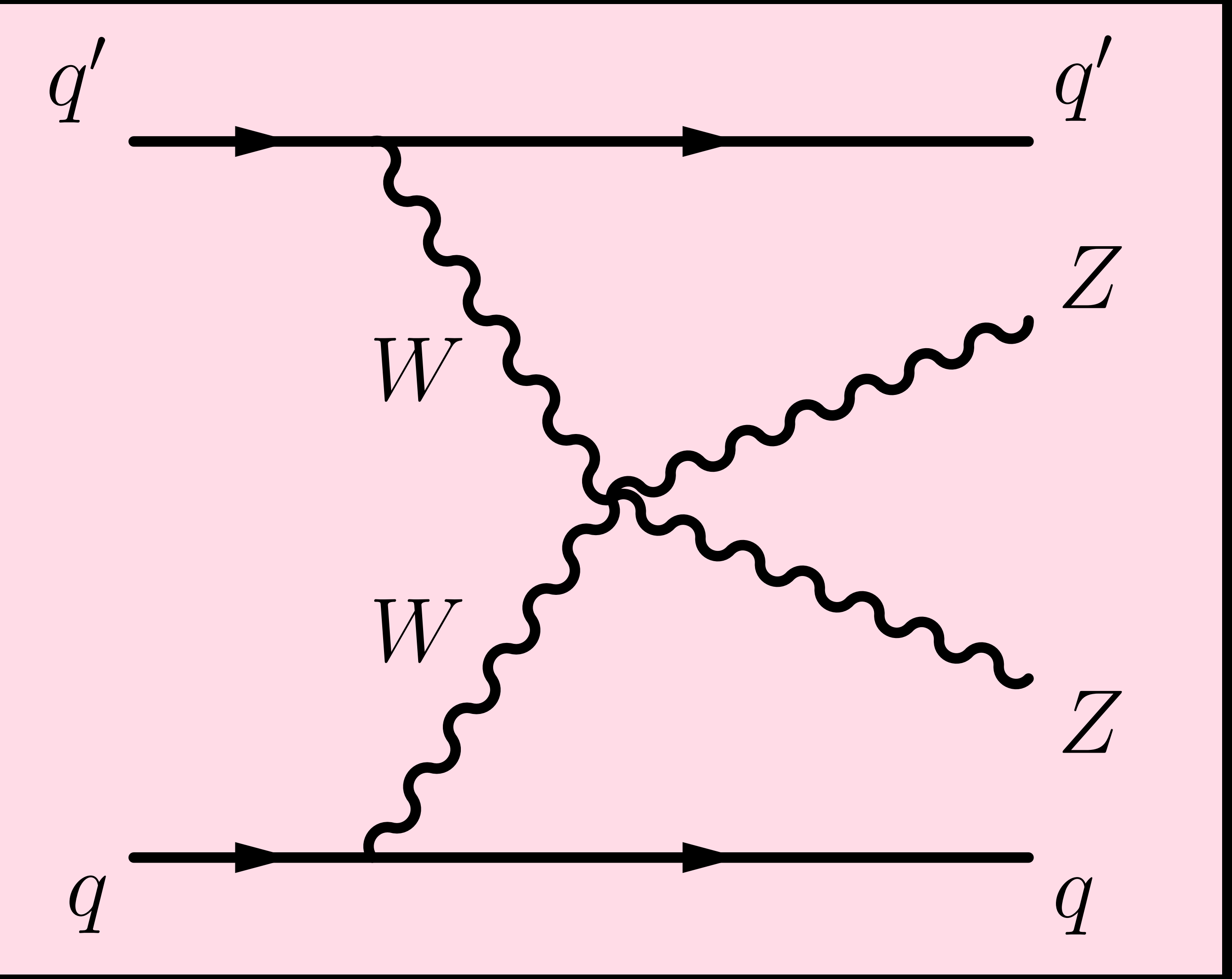

Observation of electroweak production of two jets and a Z-boson pair

- Multivariable classifier trained with (indicative) m_{jj}, p_T of the leading and sub-leading jets, p_T of the reconstructed Z-boson mass, rapidity of both Z-bosons

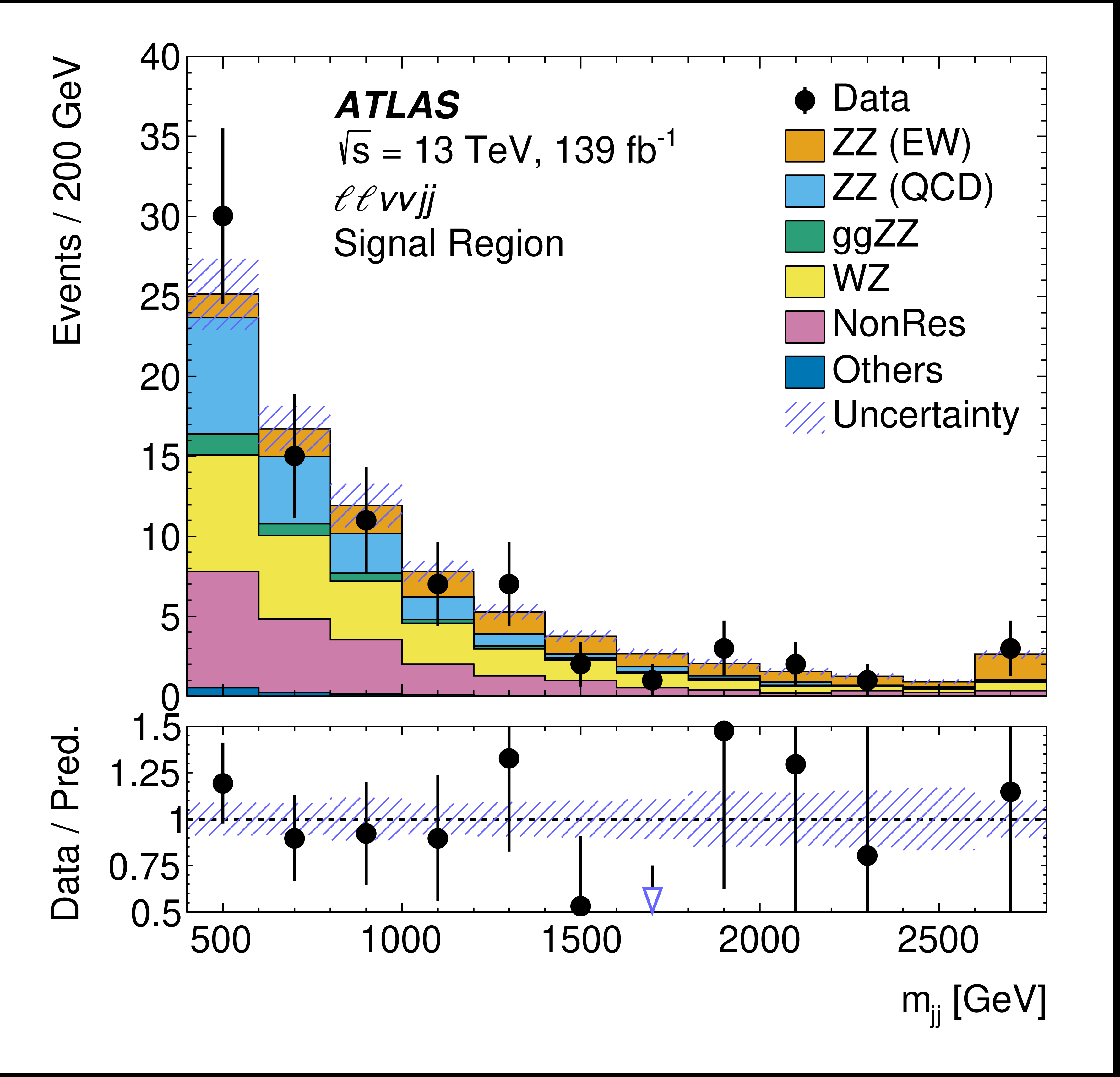

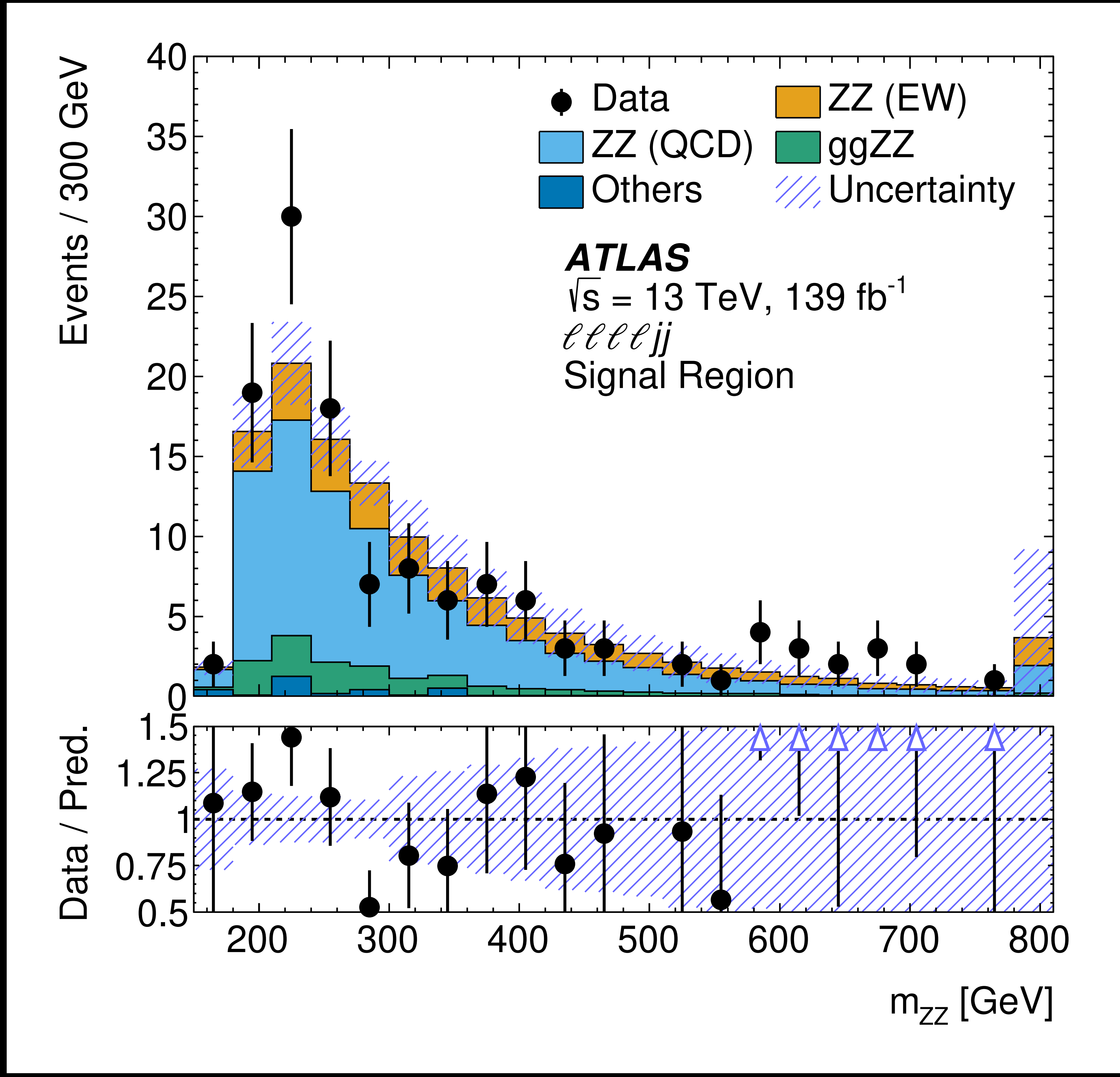

	μ_{EW}	$\mu_{QCD}^{\ell\ell\ell\ell jj}$	Significance Obs. (Exp.)
$\ell\ell\ell\ell jj$	0.97 ± 0.27	0.99 ± 0.22	5.5 (5.6) σ
$\ell\ell\nu\nu jj$	0.7 ± 0.5	–	1.3 (2.1) σ
Combined	0.92 ± 0.24	0.99 ± 0.22	5.7 (5.9) σ

Vector Boson Scattering — evolution of knowledge

CMS

$\sqrt{s}$	Process	Reference	Significance/Status
8 TeV	EW W±W±jj $(2\ell 2\nu jj)$	PhysRevLett.114.051801	2σ
	EW Zγjj $(\nu\nu/\ell\ell\gamma jj)$	PhysLettB770(2017)380-402	3σ
	EW W±γjj $(\ell\nu\gamma jj)$	JHEP06(2017)106	2.7σ
	EW W±Zjj $(3\ell\nu jj)$	PhysRevLett.114.051801	2σ
13 TeV	EW W±W±jj $(2\ell 2\nu jj)$	PhysLettB809(2020)	2016: 5.5σ, Run II ≫ 5.0σ
	EW ZZjj $(4\ell jj)$	PhysLettB812(2021)135992	2016: 2.7σ, Run II: 4.0σ
	EW W±Zjj $(3\ell jj)$	PhysLettB809(2020)135710	6.8σ
	EW Zγjj $(\ell\ell\gamma jj)$	PhysRevD.104.072001	4.7σ, Run II ≫ 5.0σ
	EW W±γjj $(\ell\nu\gamma jj)$	PhysLettB811(2020)135988	2016: 5.3σ
	EW W±Vjj $(\ell\nu jjjj)$	arXiv:2112.05259	4.4σ
	EW W±W∓jj $(2\ell 2\nu jj)$	arXiv:2205.05711	5.6σ
	EW VVpp $(4jpp)$	arXiv:2211.16320	CMS with TOTEM
	EW W±γjj	arXiv:2212.12592	Cross section measurement with full Run II

Measurement of the electroweak production of Wγ with two jets

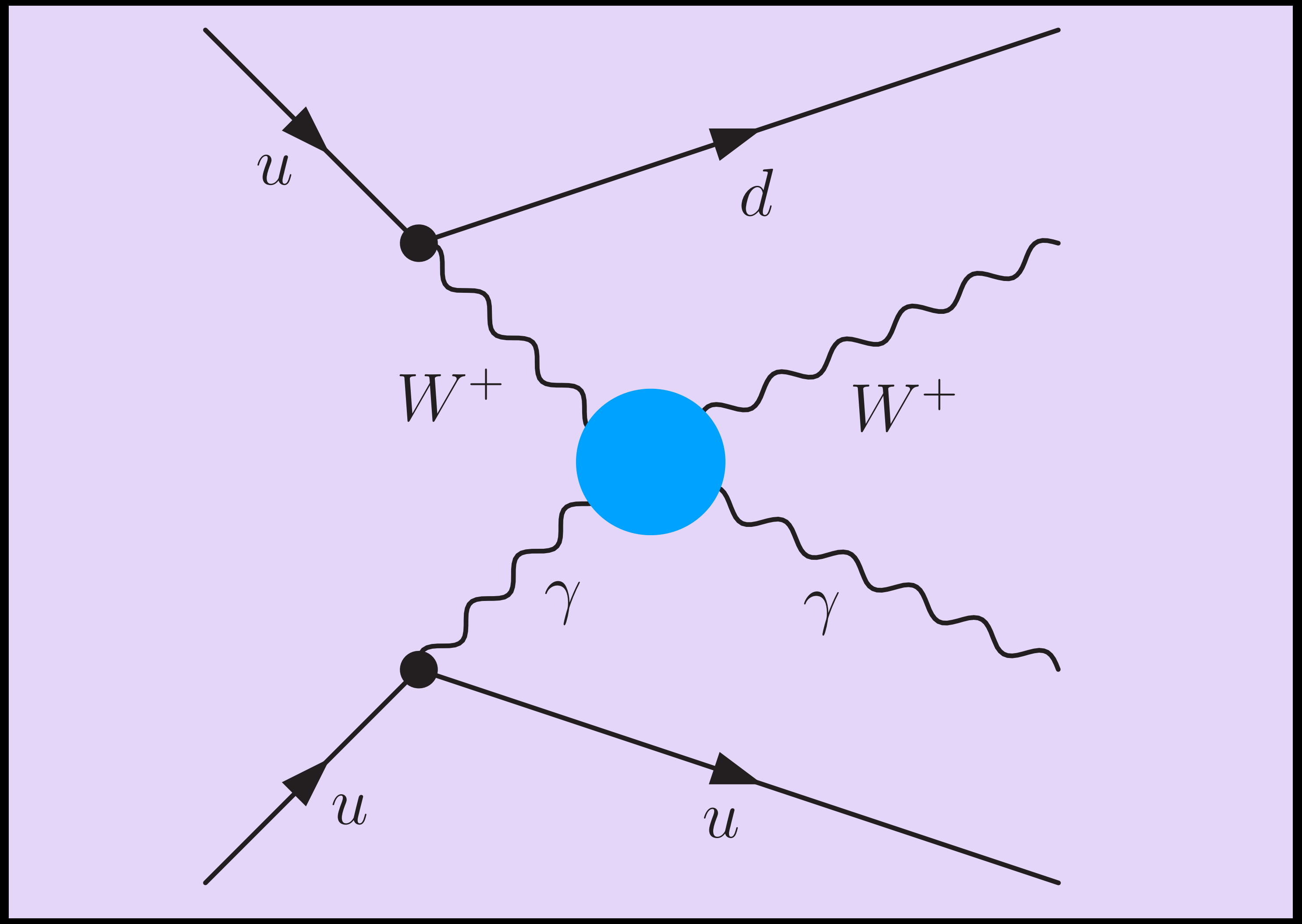

- First observation of the Wγ + 2 jets process with observed (expected) significance of 5.3 (4.8) σ with 35.9 fb^{-1}
- Extensive measurement now possible with full Run II dataset
- Exploration of dim-8 operators possible due to presence of SM quartic coupling
- Invariant mass of the Wγ system is sensitive to presence of dim-8 operators

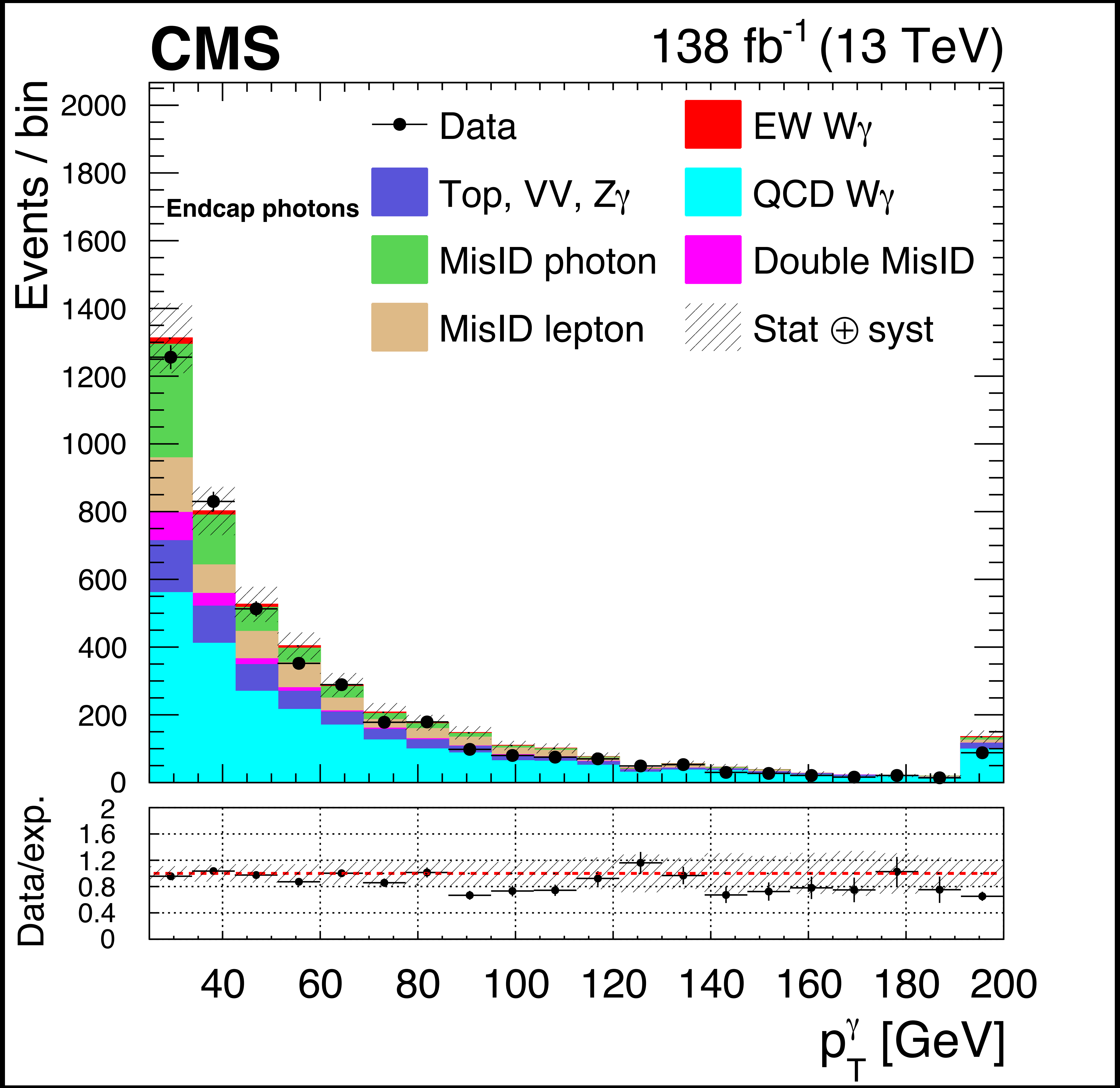

Measurement of the electroweak production of Wγ with two jets

- Major backgrounds from W+jets and $t\bar{t}$ processes where the jet constituents is misidentified as a photon

	Barrel	Endcap
EW Wγ in fiducial region	316 ± 16	90.2 ± 5.5
EW Wγ out of fiducial region	64.7 ± 2.0	20.4 ± 1.0
QCD Wγ	1301 ± 28	362 ± 13
top, VV, Zγ	402 ± 14	93.3 ± 7.2
Nonprompt photon	434 ± 13	120.2 ± 5.7
Nonprompt muon	134 ± 27	45 ± 11
Nonprompt electron	189 ± 20	86 ± 13
Nonprompt photon, nonprompt muon	43.0 ± 7.0	14.6 ± 3.4
Nonprompt photon, nonprompt electron	75.5 ± 5.5	25.0 ± 2.0
Total prediction	2960 ± 43	856 ± 21
Data	2959 ± 57	849 ± 32

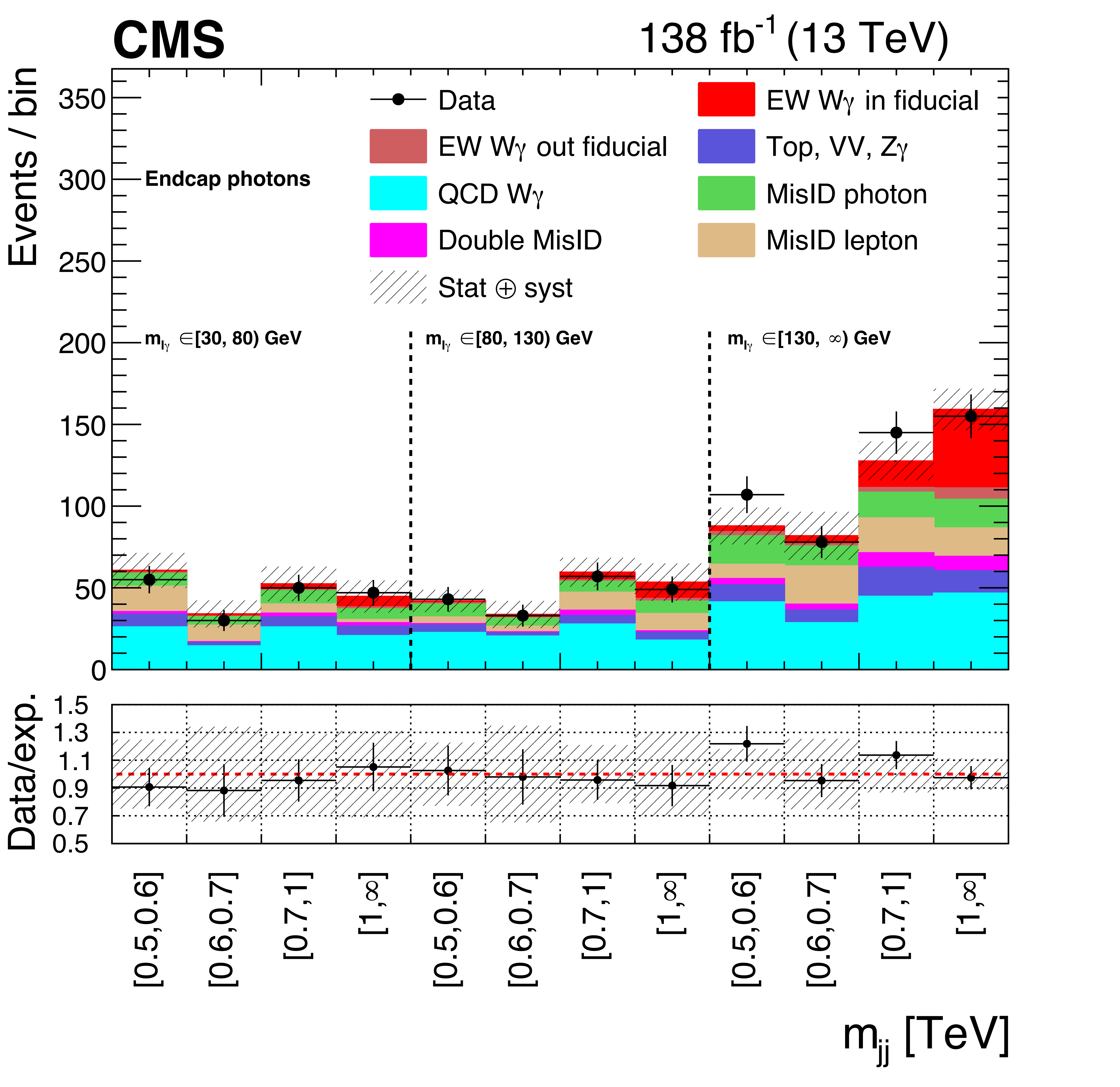

Search for exclusive $\gamma\gamma \rightarrow WW$ and $\gamma\gamma \rightarrow ZZ$ production in final states with jets and forward protons

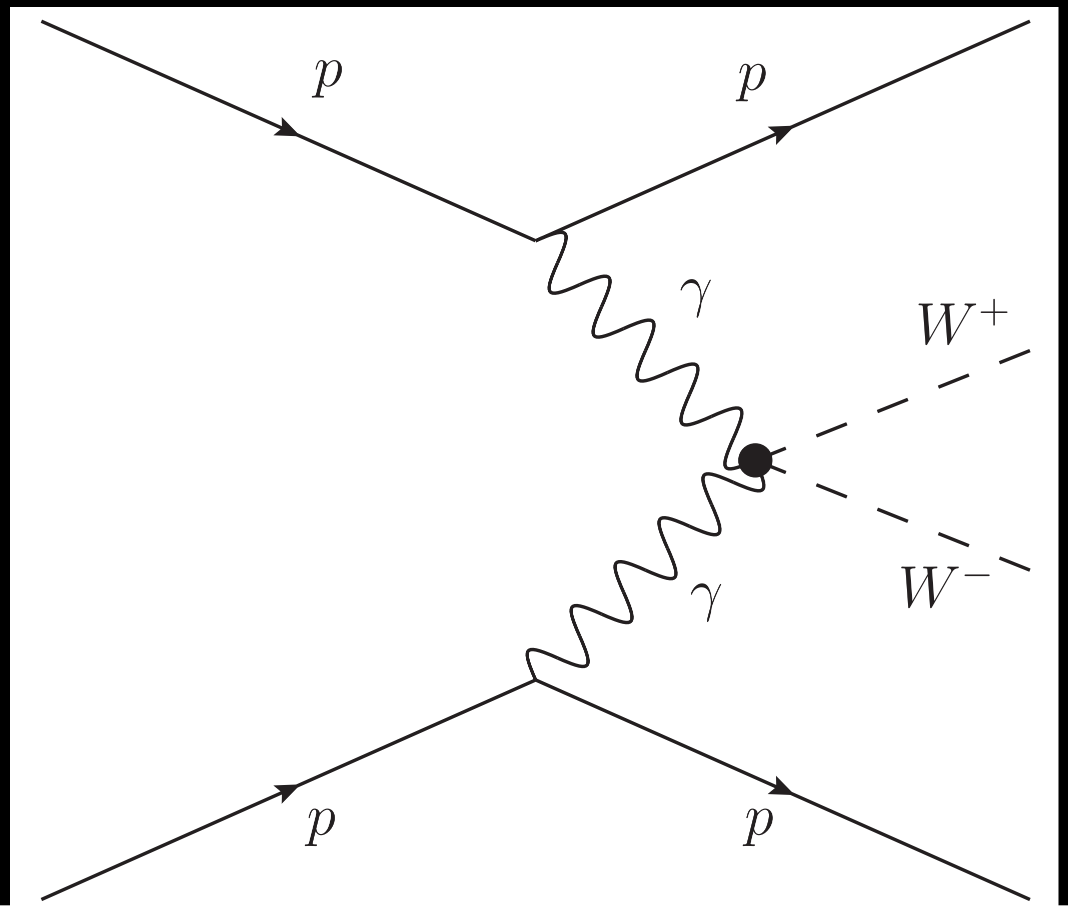

- Both protons tagged by the precision proton spectrometer (PPS)
- The $\gamma\gamma \rightarrow WW$ process allows the study of the quartic coupling
- Events selected based on properties of jets, the protons and their correlation
- First search for anomalous high-mass $\gamma\gamma \rightarrow WW$ and $\gamma\gamma \rightarrow ZZ$ using reconstructed forward protons
  - Limits 15-20x more stringent than previous results

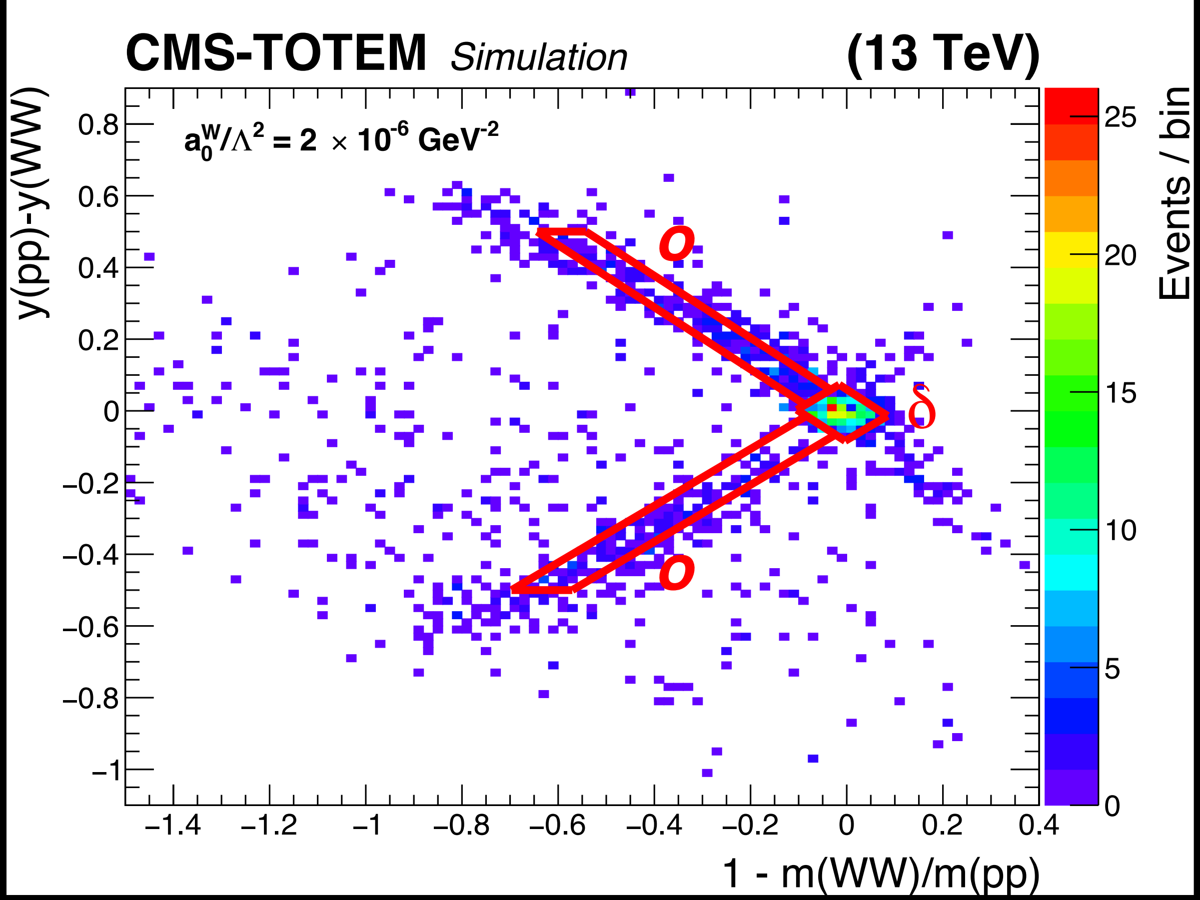

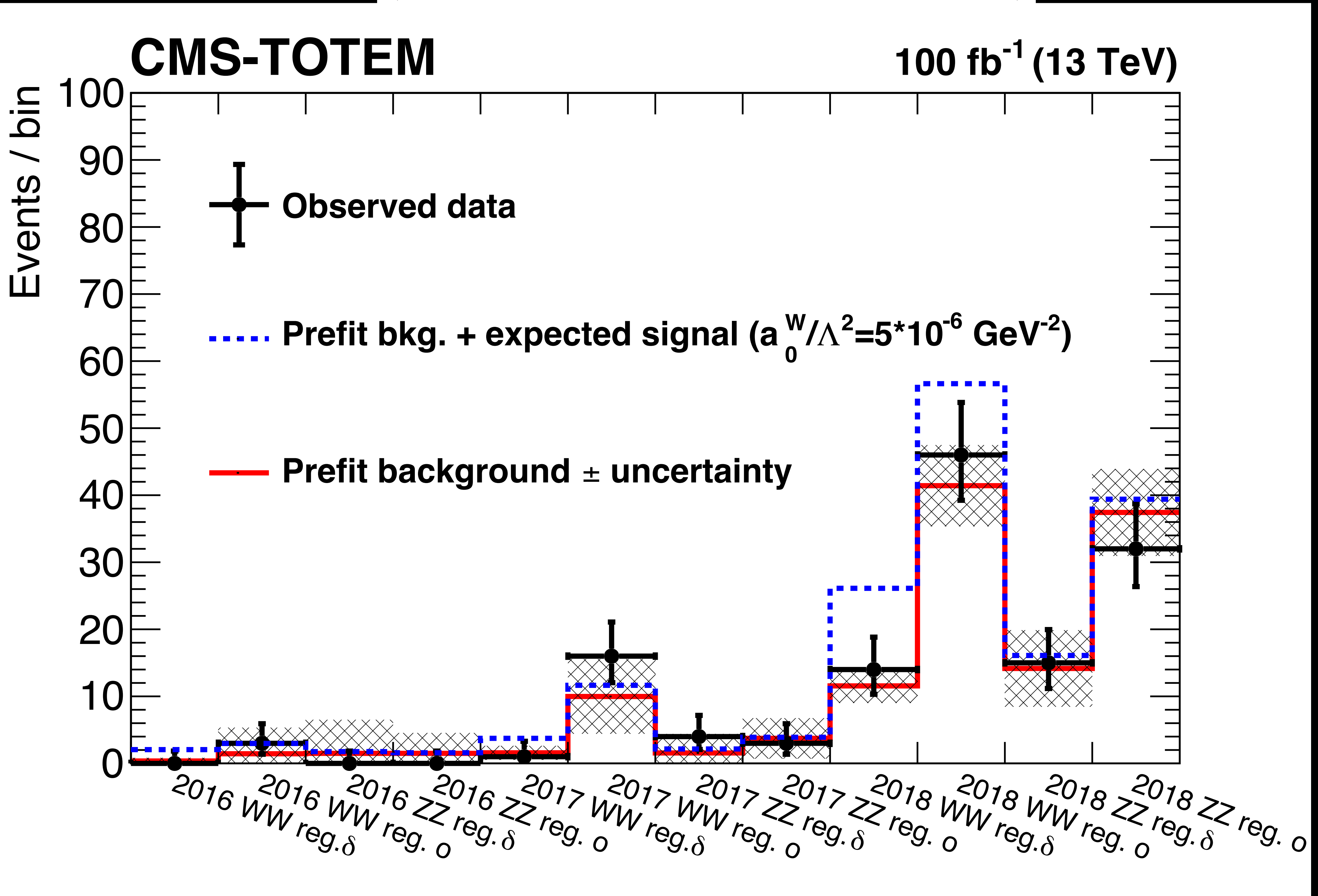

Search for exclusive $\gamma\gamma \to WW$ and $\gamma\gamma \to ZZ$ production in final states with jets and forward protons

Number of events	region	N_{evt} (2016)	N_{evt} (2017)	N_{evt} (2018)
Anti-acoplanarity sideband	δ	1.5 ± 1.1	1.6 ± 0.8	14.2 ± 3.0
Anti-pruned mass sideband	δ	0.4 ± 0.2	0.9 ± 0.2	9.9 ± 0.9
Event mixing	δ	$0.5\ (< 2.1)$	$1.5\ (< 3.6)$	11.6 ± 9.4
Expected signal ($a_0^Z/\Lambda^2 = 1 \times 10^{-5}\,\mathrm{GeV}^{-2}$)	δ	1.3	1.4	9.0
Anti-acoplanarity sideband	o	1.5 ± 1.1	3.7 ± 1.5	37.4 ± 5.6
Anti-pruned mass sideband	o	2.1 ± 0.8	5.4 ± 1.3	41.7 ± 3.1
Event mixing	o	2.0 ± 1.8	6.3 ± 5.1	42 ± 16
Expected signal ($a_0^Z/\Lambda^2 = 1 \times 10^{-5}\,\mathrm{GeV}^{-2}$)	o	1.0	1.6	12.8

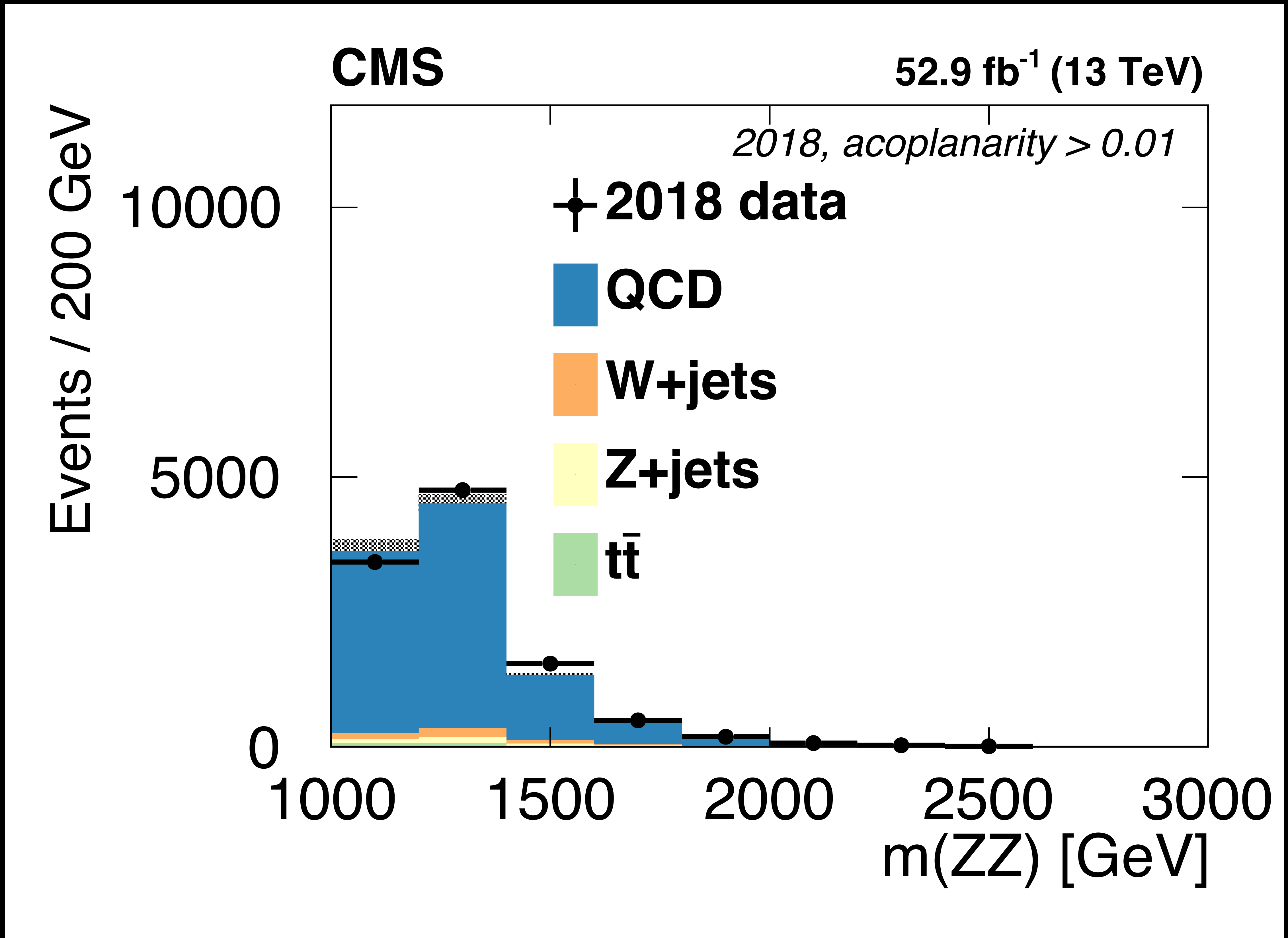

First observation of the electroweak production of a leptonically decaying W^+W^- pair in association with two jets

- First observation of W^+W^-+ 2 jets with 5.6 σ (5.2 σ) observed (expected) significance
- Require oppositely charged pair of leptons
- Major backgrounds: Drell-Yan, $t\bar{t}$
- Optimize signal significance: categorization based on the centrality of the dilepton system w.r.t. to the tagging jets
- Deep neural network (DNN) trained with (indicative):
  - M_{jj} and $\Delta\eta_{jj}$
  - $Z_{\ell_{1,2}} = \eta_{\ell_{1,2}} - \frac{1}{2}\left(\eta_{j_1} + \eta_{j_2}\right)$
- Inclusive cross section: 99 ± 20 fb

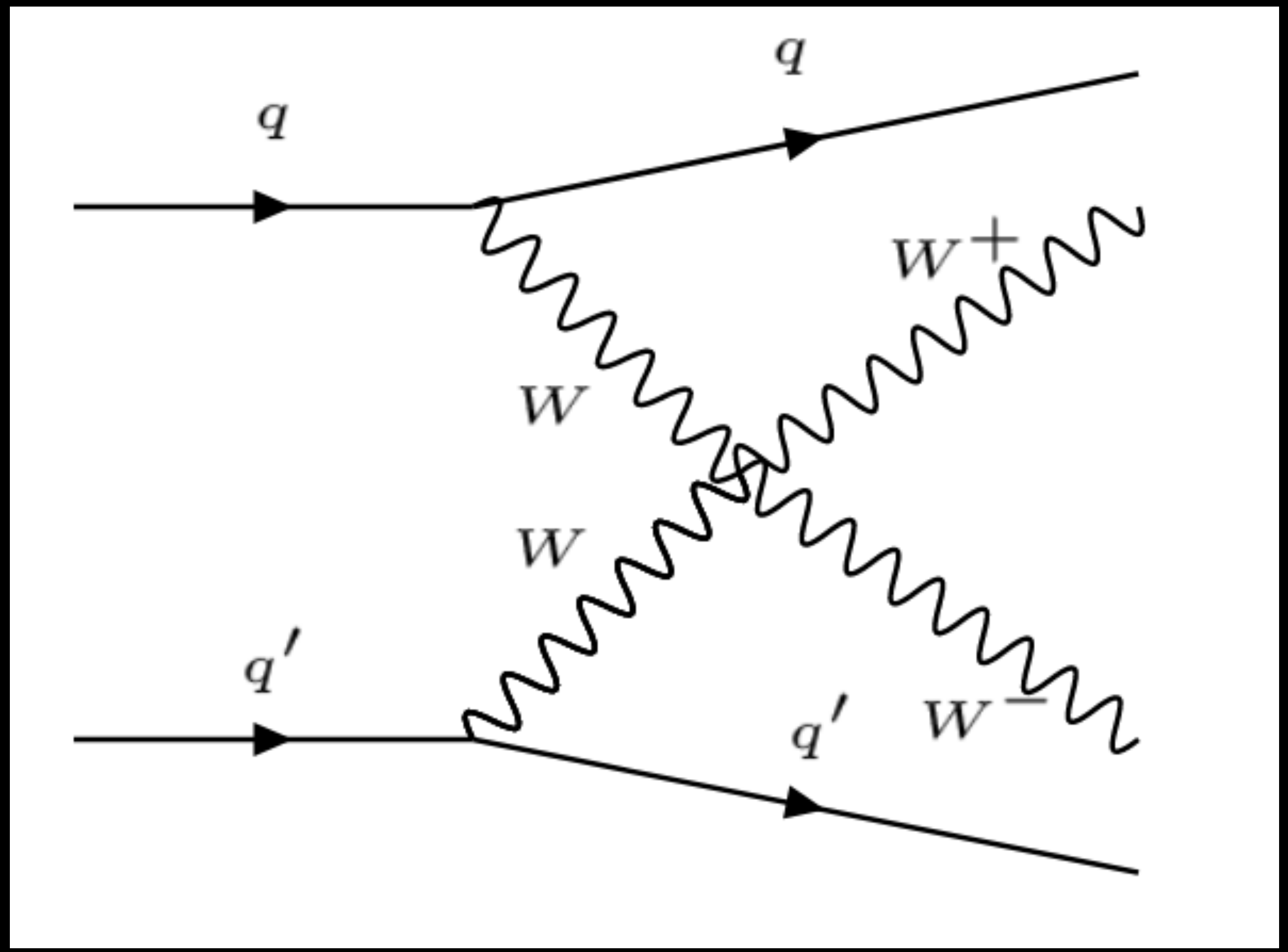

Variable	Description
m_{jj}	Invariant mass of the two tagging jets pair
$p_T^{j_1}$	p_T of the highest p_T jet
$\lvert\Delta\eta_{jj}\rvert$	Pseudorapidity separation between the two tagging jets
$p_T^{j_2}$	p_T of the second-highest p_T jet
Z_{ℓ_2}	Zeppenfeld variable of the second-highest p_T lepton
$p_T^{\ell\ell}$	p_T of the lepton pair
$\Delta\phi_{\ell\ell}$	Azimuthal angle between the two leptons
Z_{ℓ_1}	Zeppenfeld variable of the highest p_T lepton
$m_T^{\ell_1}$	Transverse mass of the $(p_T^{\ell_1}, p_T^{miss})$ system

First observation of the electroweak production of a leptonically decaying W^+W^- pair in association with two jets

- Largest uncertainty associated with QCD-induced W^+W^- normalization
- Plots below show $Z_{\ell\ell} > 1$, where $\frac{1}{2}|Z_{l_1} + Z_{l_2}|$, $Z_\ell = \eta_\ell - \frac{1}{2}(\eta_{j_1} + \eta_{j_2})$

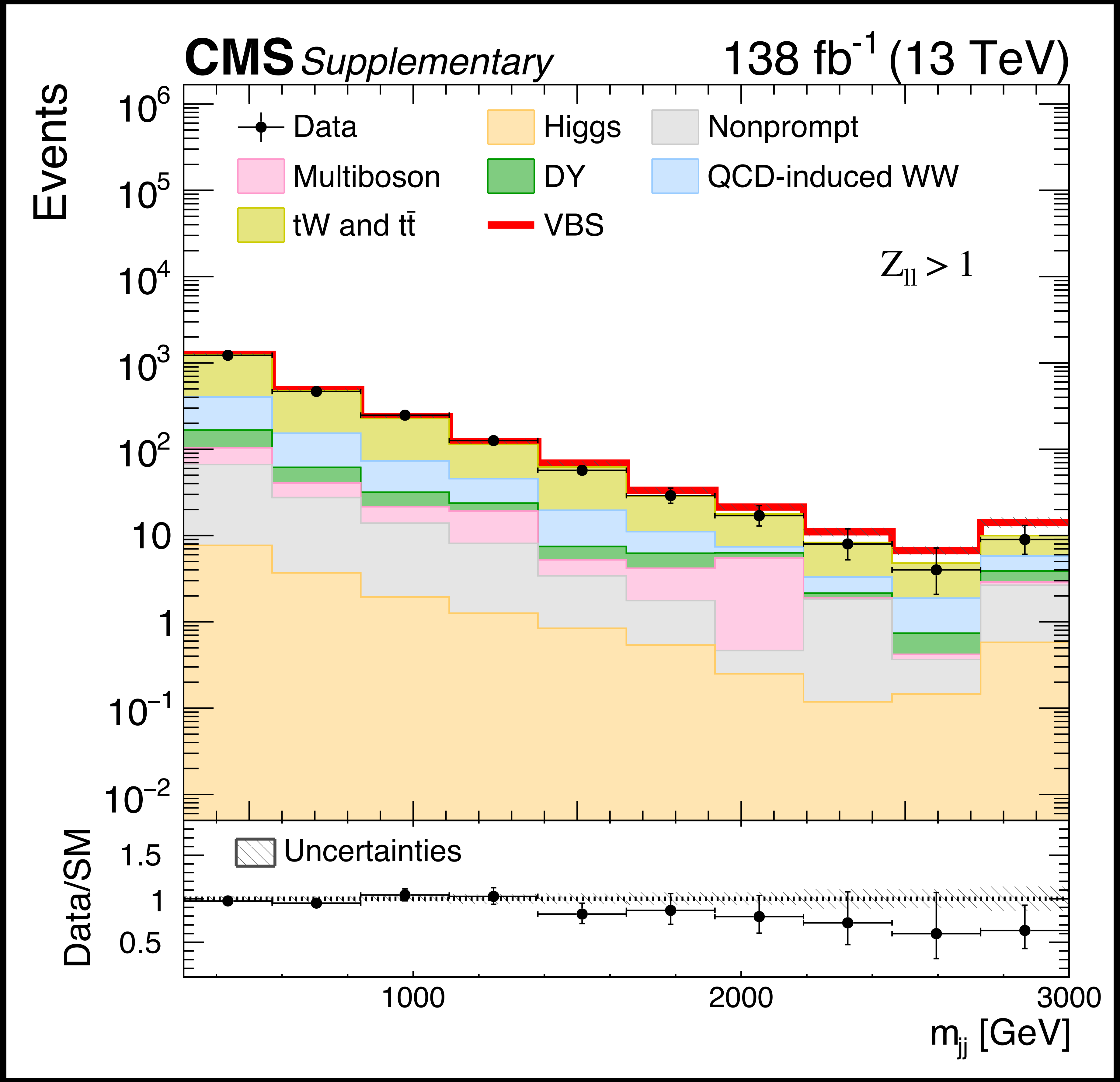

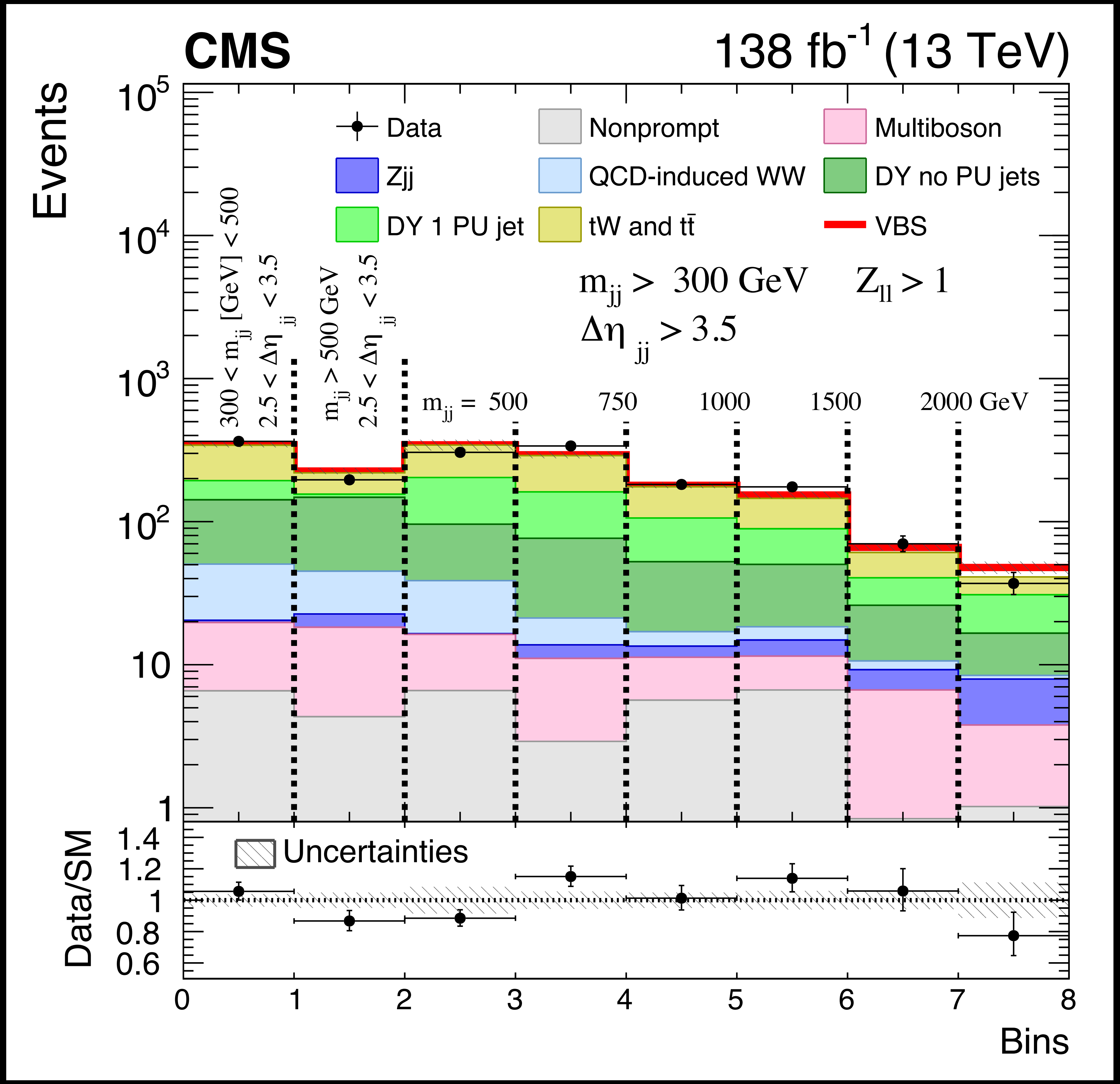

Search for vector boson scattering at the LHC Run 2 with CMS data in the semi-leptonic $\ell \nu qq$ final state

- First evidence of electroweak WW/WZ vector boson scattering ($\ell \nu qq$) with 4.4 σ (5.1 σ) observed (expected) significance
- DNN trained with (indicative):
  - Lepton η, p_T, M_{jj}
- Two different event categories:
  - based on reconstruction regime of hadronically decaying W

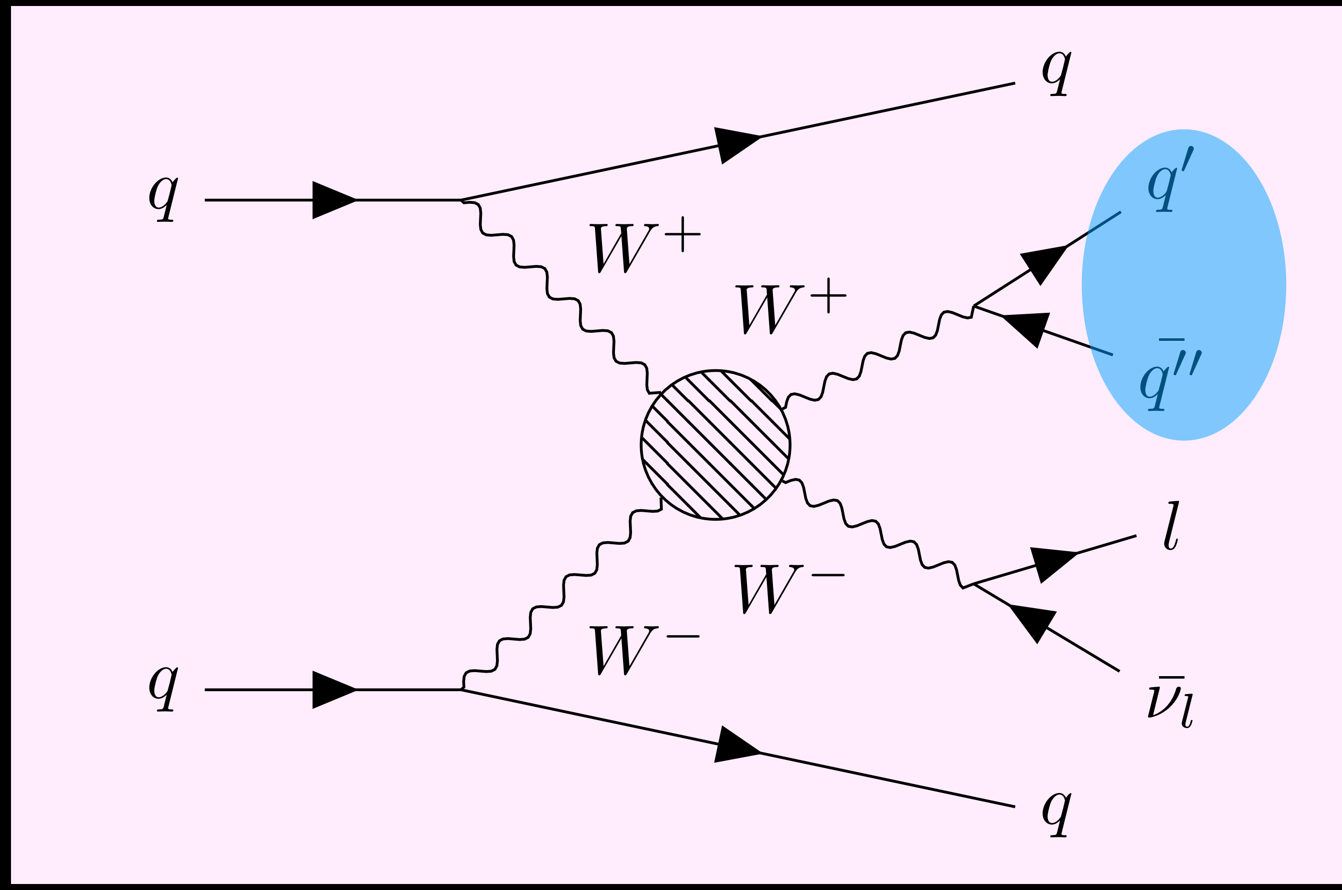

Variable	Resolved	Boosted	SHAP ranking Resolved	SHAP ranking Boosted
Lepton pseudorapidity	✓	✓	13	12
Lepton transverse momentum	✓	✓	16	10
Zeppenfeld variable for the lepton	✓	✓	2	2
Number of jets with $p_T > 30\,\text{GeV}$	✓	✓	7	3
Leading VBS tag jet p_T	-	✓	-	11
Trailing VBS tag jet p_T	✓	✓	7	6
Pseudorapidity interval $\Delta\eta_{jj}^{VBS}$ between tag jets	✓	✓	4	4
Quark/gluon discriminator of leading VBS tag jet	✓	✓	9	7
Azimuthal angle distance between VBS tag jets	✓	-	10	-
Invariant mass of the VBS tag jets pair	✓	✓	1	1
p_T of the leading V_{had} jet	✓	-	14	-
p_T of the trailing V_{had} jet	✓	-	12	-
Pseudorapidity difference between V_{had} jets	✓	-	8	-
Quark/gluon discriminator of the leading V_{had} jet	✓	-	3	-
Quark/gluon discriminator of the trailing V_{had} jet	✓	-	5	-
p_T of the AK8 V_{had} jet candidate	-	✓	-	8
Invariant mass of V_{had}	✓	✓	11	5
Zeppenfeld variable for V_{had}	-	✓	-	9
Centrality	-	✓	15	13

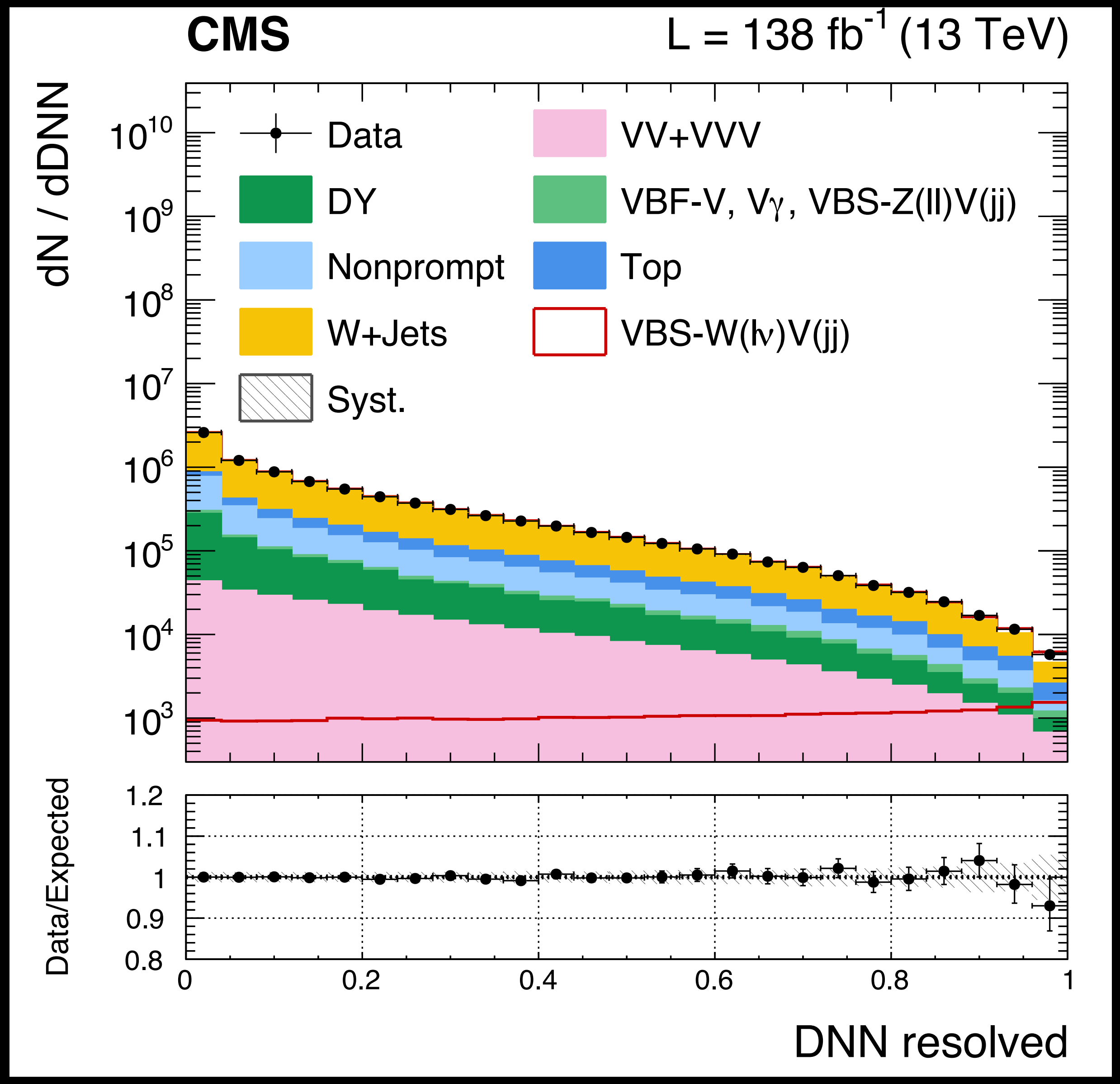

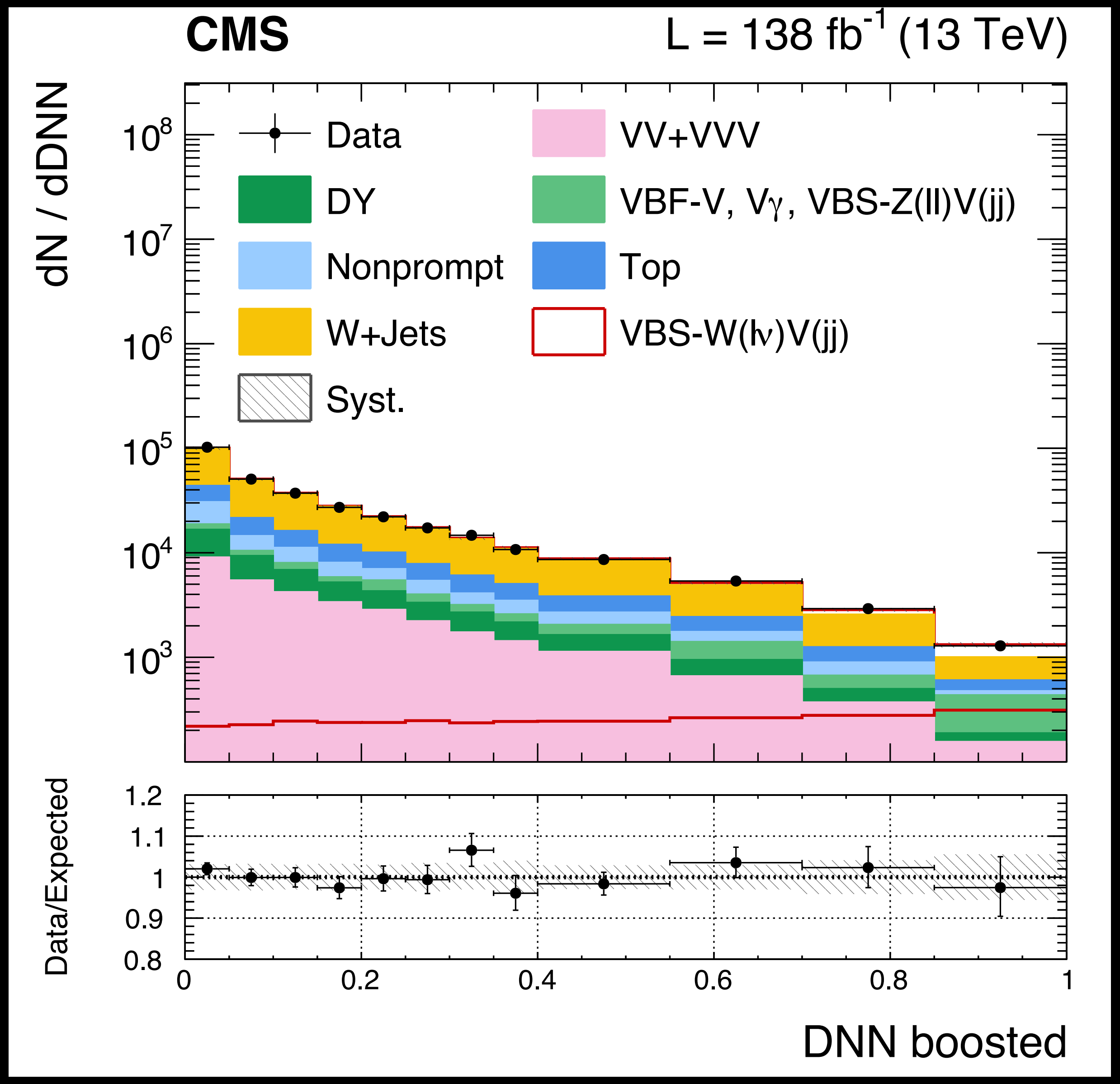

Search for vector boson scattering at the LHC Run 2 with CMS data in the semi-leptonic $\ell\nu qq$ final state

- Uncertainties arise from choice of renormalization and factorization scales
- Signal strengths associated with QCD and electro-weak production are simultaneously extracted with compatibility at 68% with SM prediction

Uncertainties associated with electro-weak VBS signal extraction

Uncertainty source	$\Delta\mu_{EW}$
Statistical	0.12
Limited sample size	0.10
Normalization of backgrounds	0.08
Experimental	
b-tagging	0.05
Jet energy scale and resolution	0.04
Integrated luminosity	0.01
Lepton identification	0.01
Boosted V boson identification	0.01
Total	0.06
Theory	
Signal modeling	0.09
Background modeling	0.08
Total	0.12
Total	0.22

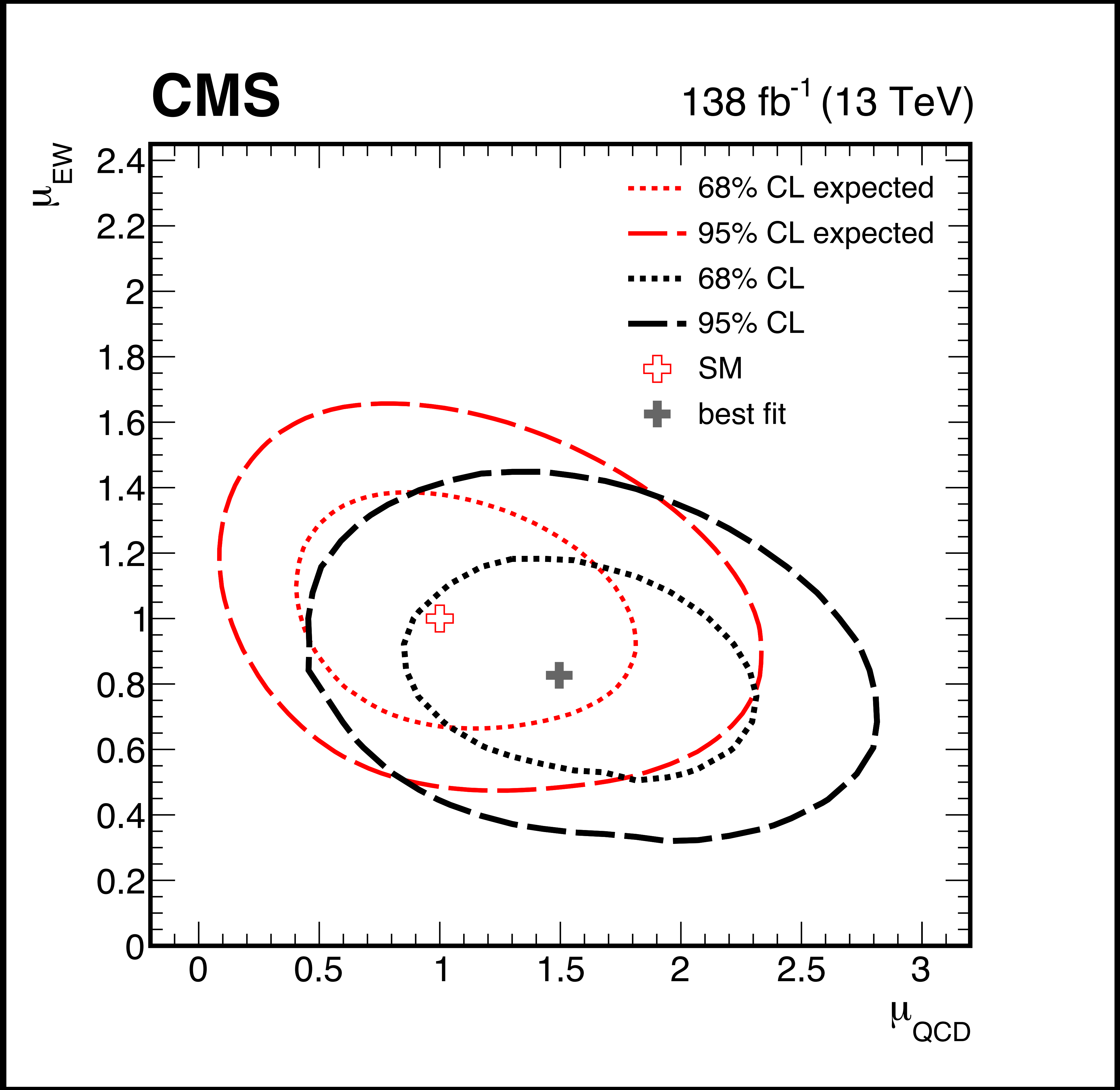

Going forward… (practicalities)

- Study of vector boson scattering processes is an exciting area of research with many new analyses in the last few years
- Run III dataset provides additional opportunities to study these processes in depth
- As the precision program of the LHC is realized, studying generator modeling is crucial
  - Many different generators studied with various configurations
    - Features discussion of choice of dipole recoil scheme
    - Synchronize sample production between ATLAS and CMS

Sample name	Generator	μ-scale	Shower	Tune	PDF	further settings
Sherpa (ATLAS)	SHERPA v2.2.2	dynamic scale, m_{WW}	internal	internal	NNPDF3.0-NNLO	multileg-LO, exactly six EW vertices with one additional parton at LO accuracy in QCD
PW+Py8 (ATLAS)	POWHEG v2, VBS approx.	fixed scale, m_W	PYTHIA 8.212	AZNLO	NNPDF3.0-NLO	NLO
PW+Py8 dipole-recoil (ATLAS)	POWHEG v2	fixed scale, m_W	PYTHIA 8.235	AZNLO	NNPDF3.0-NLO	Dipole Recoil [6]
MG5+Py8 dipole-recoil (ATLAS)	MG5_AMCNLO v2.6.2	dynamic scale, $\sqrt{p_T^{jet1} p_T^{jet1}}$	PYTHIA 8.235	A14	NNPDF3.0-NLO	LO, Dipole Recoil [6]
MG5+Py8 (CMS)	MG5_AMCNLO v2.3.3	dynamic scale, using a 2→2 topology from the clustered external state	PYTHIA 8.212	CUETP8M1 [7]	NNPDF3.0-LO	LO, exactly six EW vertices
PW+Py8 (VBScan)	POWHEG v2	dynamic scale, $\sqrt{p_T^{jet1} p_T^{jet2}}$	PYTHIA 8.230	Monash	NNPDF3.0-NLO	NLO

Going forward…

CMS-PAS-FTR-21-001

- Understanding electroweak symmetry breaking → crucial part of LHC physics program
  - Longitudinally polarized scattering of W and Z complementary to direct measurements of the Higgs coupling to gauge bosons
- Analysis projected from Run II to 3000 fb^{-1}

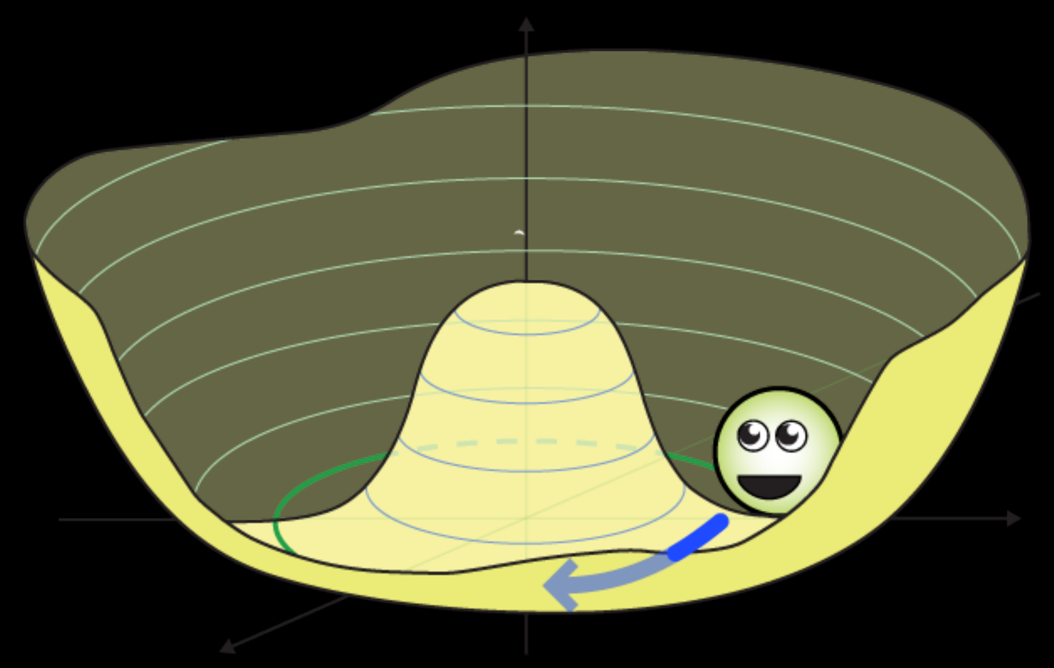

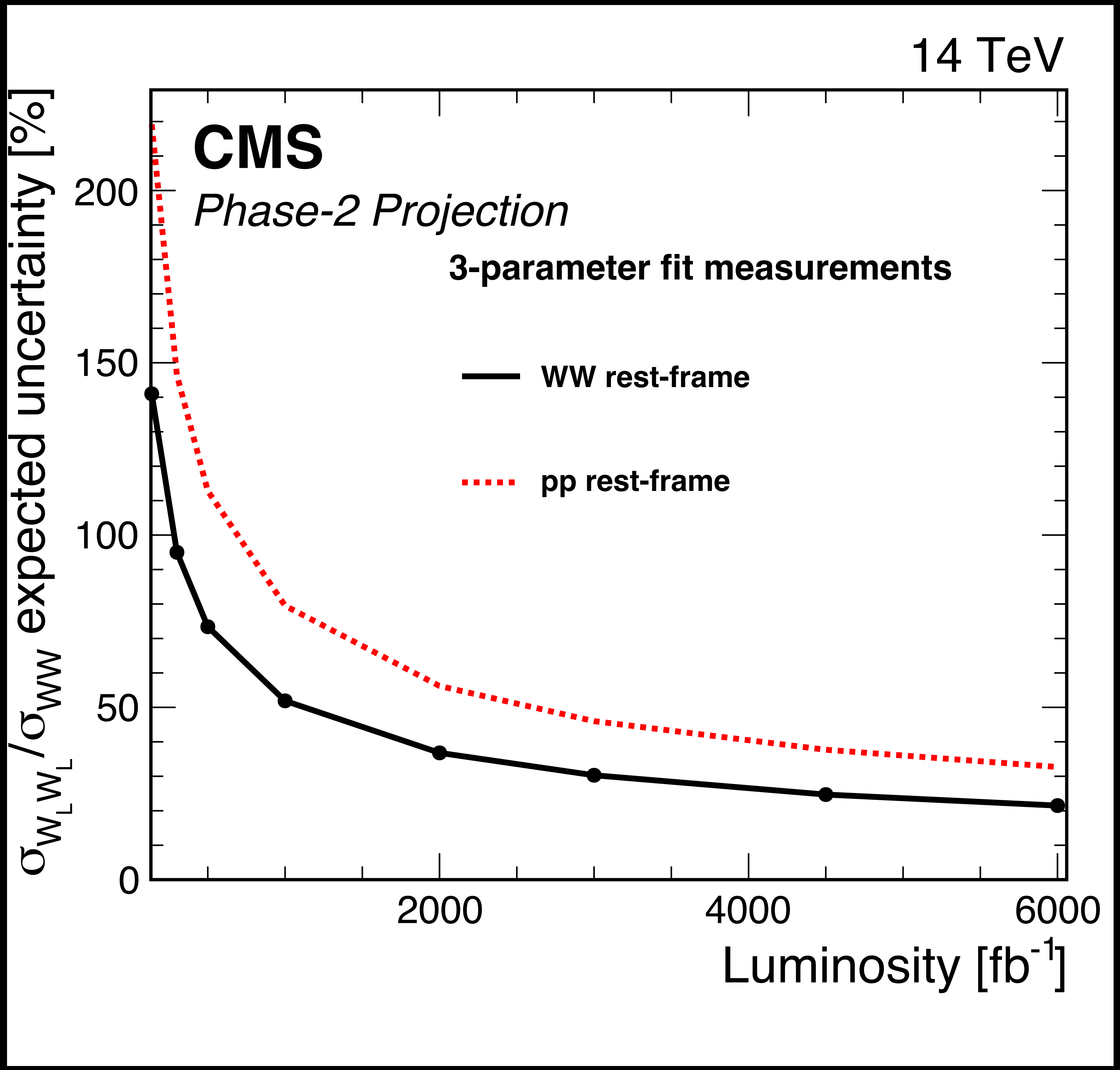

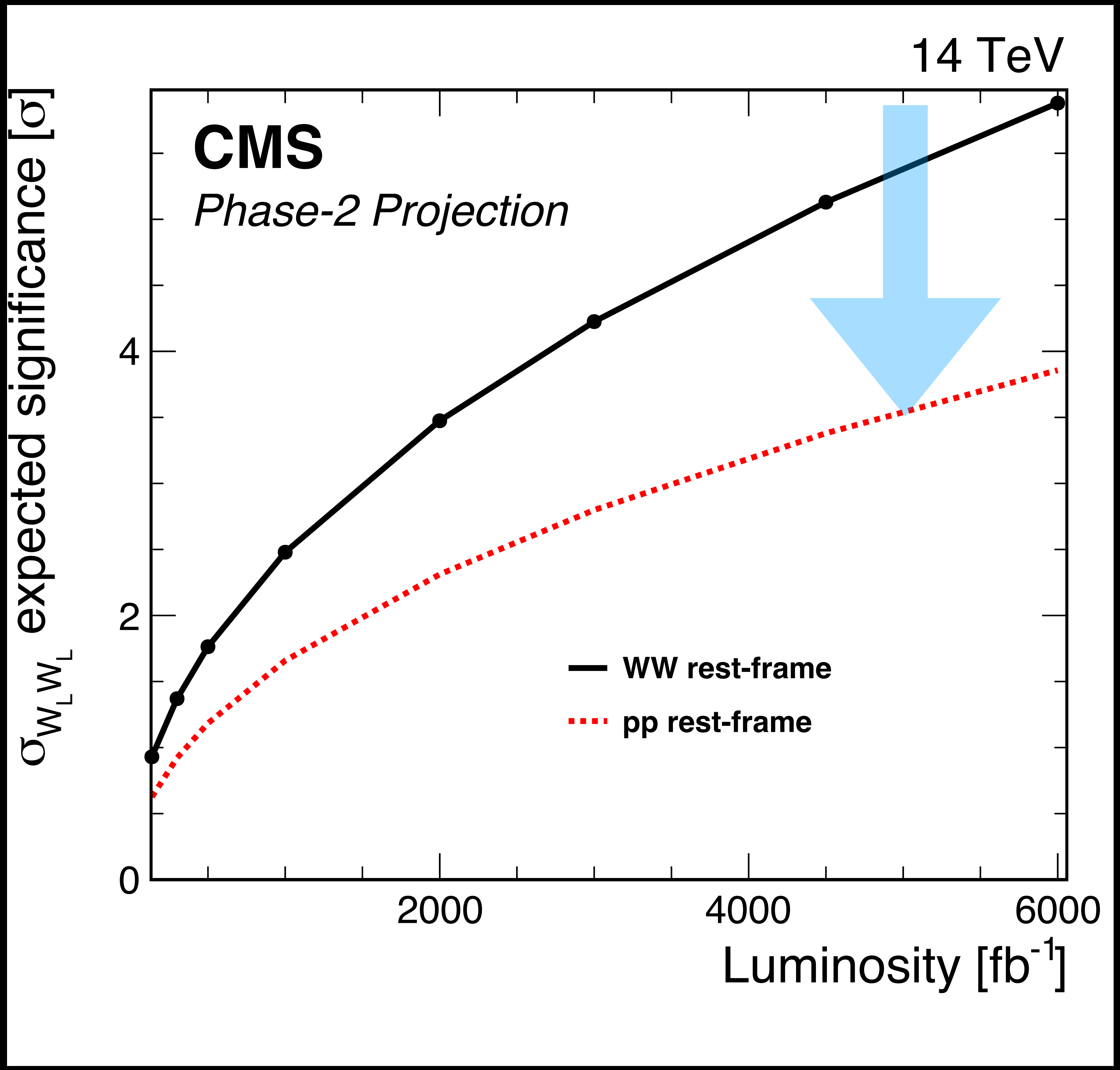

Additional Material

arXiv:2305.19142

Furthermore, to enhance the VBS topology, events must have at least two jets with p_T^j above 50 GeV and a rapidity difference between them, $|\Delta y| > 1$. The invariant mass of this pair of jets, m_{jj}, is required to be greater than 150 GeV for the total $Z\gamma jj$ process measurements, and greater than 500 GeV for the $Z\gamma jj$ electroweak process measurements. This selection significantly reduces the number of events with three bosons in the final state in first case, and the number of QCD $Z\gamma jj$ background events in the second case. Events containing b-tagged jets are rejected. The b-tagging algorithm provides a working point with a 70% selection efficiency for b-jets in an inclusive $t\bar{t}$ MC sample and rejection factors of ≈ 10 and 400 for charm- and light-flavour jets, respectively [43]. The two highest-p_T jets satisfying these conditions are referred to as VBS tagged jets. Events with additional jets of transverse momentum above 25 GeV in the rapidity gap between the two VBS tagged jets are rejected. The centrality of the $\ell^+\ell^-\gamma$ system relative to the VBS tagged jets (j_1 and j_2) defined as

$$\zeta(Z\gamma) = \left| \frac{y_{Z\gamma} - (y_{j_1} + y_{j_2})/2}{y_{j_1} - y_{j_2}} \right|, \tag{1}$$

where y indicates the rapidity, is required to be less than 5.

For the signal extraction the selected events are further split into a signal region (SR, $\zeta(Z\gamma) < 0.4$) and a QCD control region (CR, $\zeta(Z\gamma) > 0.4$) as explained in Section 7. For the measurements of the full $Z\gamma jj$ process, only the region $\zeta(Z\gamma) < 0.4$, referred to as 'Extended SR', is used.

The observed total number of events in the $m_{jj} > 500$ GeV SR and CR is 562 and 274 respectively. In the $m_{jj} > 150$ GeV Extended SR phase space, the observed total number of events is 1461.